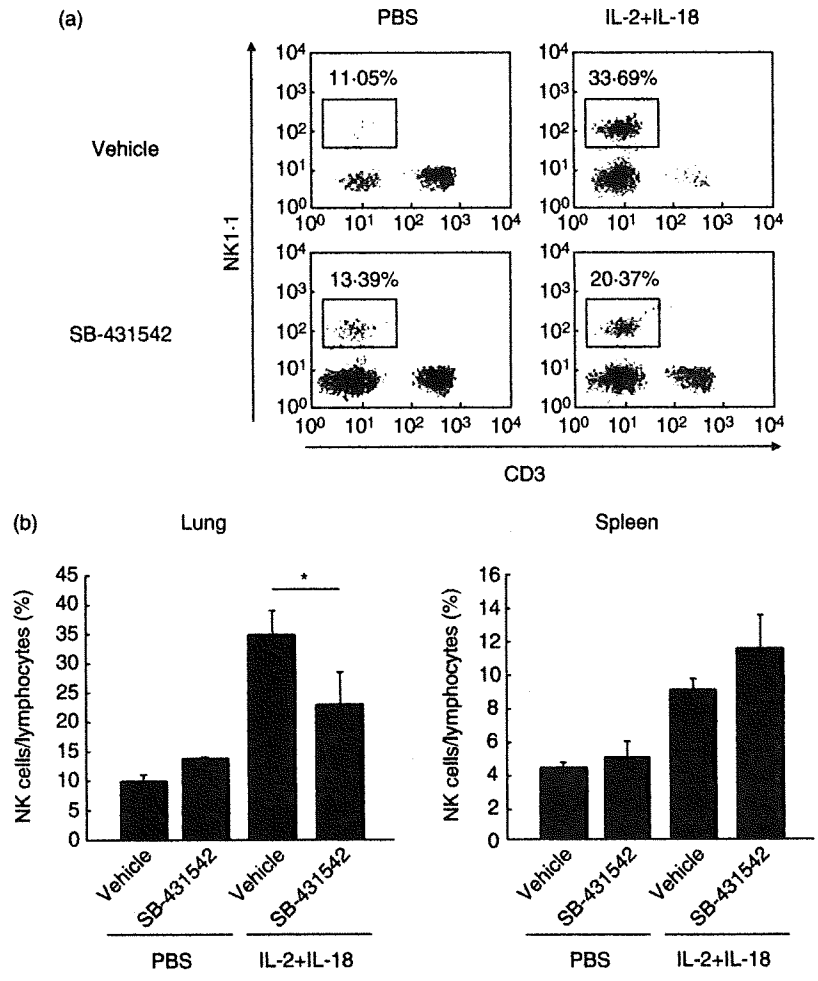

Fig. 4. Flow cytometric analysis of pulmonary lymphocytes in B6 mice treated with SB-431542. (a) Pulmonary lymphocytes were harvested from B6 mice at 24 h after treatment with interleukin (IL)-18/IL-2 with or without SB-431542 for 3 days, as described in Materials and methods. Pulmonary lymphocytes were stained with phycoerythrin (PE)-conjugated anti-natural killer (NK)1·1 and PE/cyanine 7 (Cy7)-conjugated anti-CD3ε monoclonal antibodies. (b) Left: proportion of NK cells relative to pulmonary lymphocytes in mice treated with IL-18/IL-2 and with or without SB-431542. Right: proportion of NK cells relative to splenocytes in B6 mice treated with IL-18/IL-2 with or without SB-431542. Data are mean ± standard error of the mean of three mice per group. $^*P < 0{\cdot}05$; Student's *t*-test.

SB-431542 ameliorates lowers percentage of phosphorylated Smad3-positive cells

Furthermore, the number of phosphorylated Smad3-positive cells was lower in the lung of B6 mice treated with SB-431542 compared with the control (Fig. 3a). To confirm this result, we counted the percentage of p-Smad3-positive cells relative to the total number of cells. The percentage of p-Smad3-positive cells was significantly lower in SB-431542-treated ILD mice (24·98 ± 6·11%) compared with the control (41·12 ± 4·92%, $P < 0{\cdot}05$, Fig. 3b).

SB-431542 significantly reduces NK cells in the lung

The results showed significantly fewer NK cells (22·53 ± 5·90%) in the lungs of SB-431542-treated B6 mice compared with the control (34·84 ± 4·43%, $P < 0{\cdot}05$, Fig. 4a and b). In contrast, the percentage of NK cells in splenocytes of SB-431542-treated B6 mice (11·50 ± 2·13%) tended to be higher than the control (8·99 ± 0·82%, Fig. 4b).

Improvement of ILD and reduced cell infiltration in lungs of Smad3$^{-/-}$ mice

We also conducted experiment in Smad3$^{-/-}$ mice for further assessment of the role of TGF-β signalling on IL-18/IL-2-induced ILD [31]. Histological examination showed milder cell infiltration in the lungs of Smad3$^{-/-}$ mice compared with the control (Fig. 5a). Furthermore, flow cytometry showed a significantly small proportion of NK cells in the lung of Smad3$^{-/-}$ mice treated with IL-18/IL-2 (22·77 ± 3·27%) compared with B6 mice (33·89 ± 5·06%, $P < 0{\cdot}05$, Fig. 5b and c).

Underexpression of chemokine mRNAs in lung of SB-431542-treated and Smad3$^{-/-}$ mice

RT-PCR showed that the expression levels of CCL2, CCL3, CCL4, CCL5 and CXCL10 mRNAs were lower in the lungs of B6 mice treated with SB-431542 than the control (Fig. 6a). Furthermore, the expression levels of CCL2, CCL3, CCL4, CCL5, CCL11, CXCL1 and CXCL10 were lower in the lungs of Smad3$^{-/-}$ mice than the control (Fig. 6b).

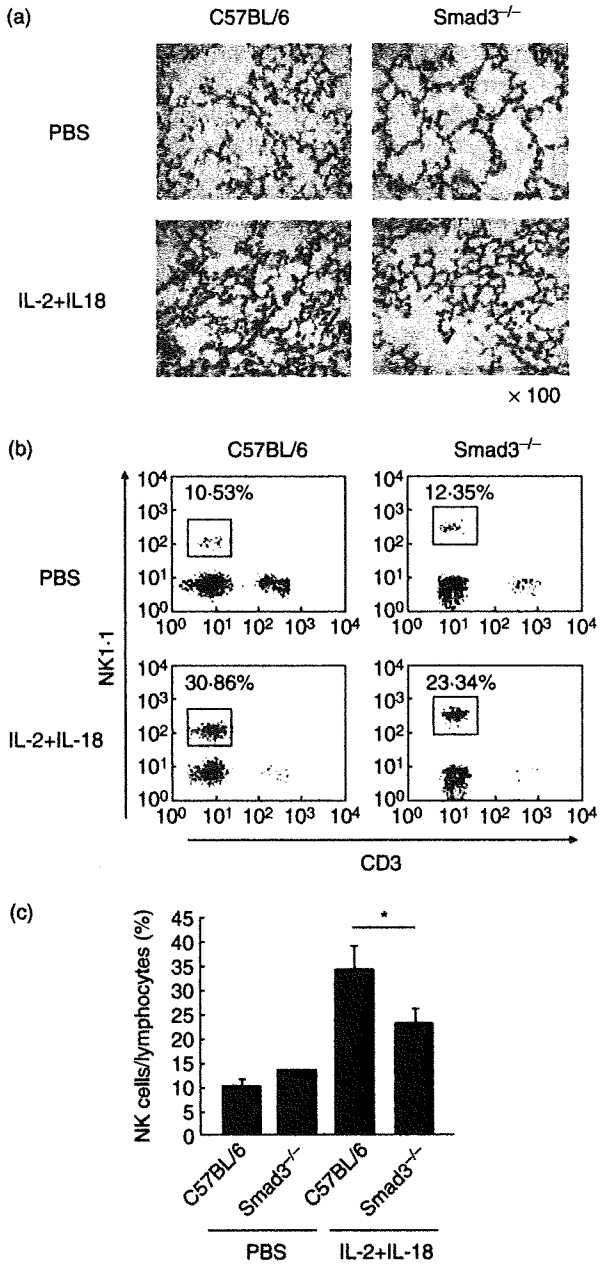

Fig. 5. Histological and flow cytometric analysis of pulmonary lymphocytes in Smad3$^{-/-}$ mice. (a) Lungs were harvested from B6 and Smad3$^{-/-}$ mice at 24 h after treated with interleukin (IL)-18/IL-2 for 3 days. Lung tissues were stained with haematoxylin and eosin. Original magnification: ×100. (b) Pulmonary lymphocytes were harvested from B6 and Smad3$^{-/-}$ mice at 24 h after treatment with IL-18/IL-2 for 3 days, as described in Materials and methods. Pulmonary lymphocytes were stained with phycoerythin (PE)-conjugated anti-natural killer (NK)1·1 and PE/cyanine 7 (Cy7)-conjugated anti-CD3ε monoclonal antibodies. (c) Proportion of NK cells relative to pulmonary lymphocytes in B6 and Smad3$^{-/-}$ mice treated with IL-18/IL-2. Data are mean ± standard error of the mean of three mice per group. *$P < 0.05$; Student's t-test.

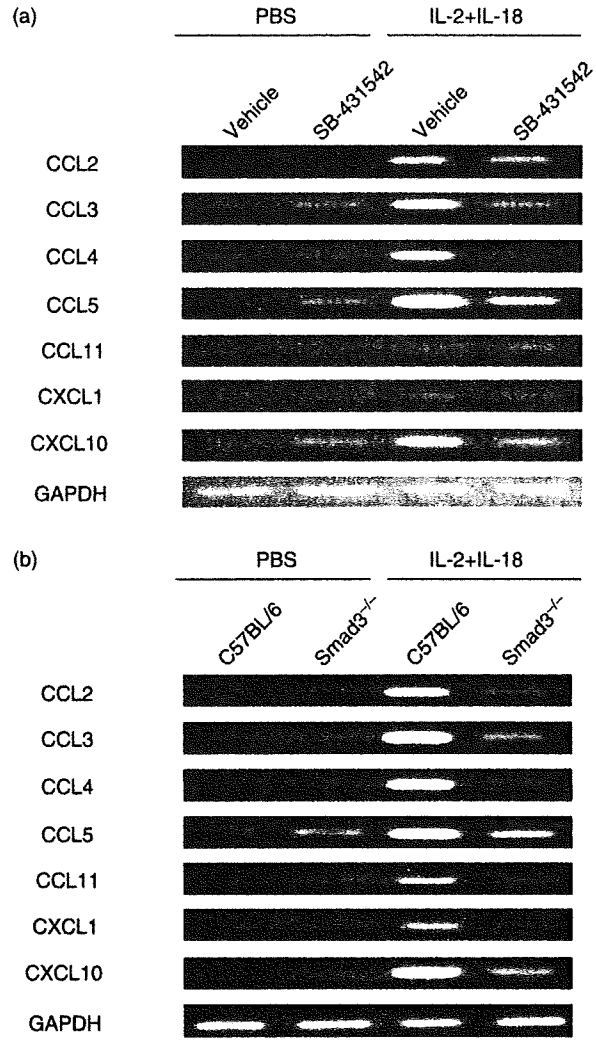

Fig. 6. Expression of chemokine mRNAs in lungs of mice deficient in transforming growth factor (TGF)-β. (a) mRNA expression of various chemokines in the lungs of B6 mice treated with SB-431542 and control mice. Lungs were removed at 24 h after the final dose of SB-431542 or vehicle and total RNA was extracted. Chemokine expression (CCL2, CCL3, CCL4, CCL5, CCL11, CXCL1 and CXCL10) was detected by reverse transcription polymerase chain reaction (RT-PCR). (b) mRNA expression of various chemokines in the lungs of Smad3$^{-/-}$ mice and control mice. Lungs were removed at 24 h after the third injection of interleukin (IL)-18/IL-2 and total RNA was extracted. Chemokine expression (CCL2, CCL3, CCL4, CCL5, CCL11, CXCL1 and CXCL10) was detected by RT-PCR. Representative results are shown of three experiments with similar findings.

Discussion

IL-18 and IL-2 are important cytokines that can induce IFN-γ production by NK cells [11]. IL-18 and IL-2 administered daily acted synergistically to induce ILD. ILD mice show severe infiltration of NK cells in the lungs and have high levels of IFN-γ in both serum and lung [19]. Depletion of NK cells by anti-NK1·1 monoclonal antibody or anti-asialo GM1 antibody treatment prevented this effect. Furthermore, the morbid effects of IL-18 and IL-2 were reduced in IFN-γ-deficient mice. These findings suggest that the increase of NK cells and elevation of IFN-γ seem to play a role in the pathogenesis of IL-18/IL-2-induced ILD in mice.

In other mouse models of ILD, BLM induces pulmonary fibrosis and the TGF-β pathway plays an important role in the pathogenesis of ILD [24,27–29,36]. The present study also showed increased expression of TGF-β mRNA in the lung in the early stage of ILD after injection of IL-18/IL-2. Thus, TGF-β seems to be involved in the pathogenesis of IL-18/IL-2-induced ILD and BLM-induced pulmonary fibrosis. Surprisingly, mice treated with SB-431542 delayed mortality in IL-18/IL-2-induced ILD. In addition, IL-18/IL-2-induced NK cell infiltration in the lung was decreased significantly following treatment with SB-431542 and also in Smad3$^{-/-}$ mice. Histological analysis demonstrated that SB-431542 reduced cell infiltration significantly in ILD mice. It was reported that injection of IL-18/IL-2 induced the expression of IFN-γ and TNF-α in sera, and IFN-γ and IL-6 in the lung [19]. In the lung, treatment with SB-431542 reduced the expression of IFN-γ and IL-6 from IL-18/IL-2-induced ILD mice, but in sera the expression of IFN-γ and TNF-α was not changed. Furthermore, IL-18/IL-2-induced ILD was improved in Smad3$^{-/-}$ mice. These findings indicate the involvement of Smad-mediated TGF-β signalling in the pathogenesis of murine ILD.

Bellone *et al.* [37] reported that TGF-β inhibited activated NK cells *in vitro*. Our preliminary study confirmed that exogenously added TGF-β suppressed NK cells *in vitro* (data not shown). However, in the present study, we demonstrated that shutdown of TGF-β signalling by SB-431542 or Smad3 knock-out down-regulated NK cells migration into the lung *in vivo*, indicating that TGF-β enhanced the infiltration of NK cells into the lung. The discrepancy might be due to the difference between the effects of TGF-β on NK cells *in vitro* and those *in vivo*. We proposed that TGF-β could enhance the migration of NK cells into the lung *in vivo*, whereas TGF-β suppressed the proliferation of NK cells *in vitro*.

Okamoto *et al.* [19] showed that certain chemokines, such as CCL2, CCL3, CCL4, CCL5, CCL11, CXCL1 and CXCL10, were up-regulated in the lungs of IL-18/IL-2-induced ILD mice. In contrast, in the lungs of B6 mice treated with SB-431542 and in Smad3$^{-/-}$ mice, chemokine mRNAs were down-regulated. Interestingly, larger proportions of NK cells were noted in the spleens of SB-431542-treated mice with ILD, although their proportion in the lungs was reduced. The latter finding may be due to redistribution and accumulation of NK cells in the spleen. Thus, inhibition of TGF-β signalling could, potentially, be a useful therapeutic strategy in ILD through regulation of NK cells infiltration in the lung.

In conclusion, the present study showed that inhibition of TGF-β signalling regulated IL-18/IL-2-induced ILD through inhibition of NK cells and down-regulation of certain chemokines in the lung. These findings support the notion that TGF-β signalling plays an important role in the pathogenesis of ILD.

Acknowledgements

We thank Dr Chuxla Deng (National Institute of Diabetes and Digestive and Kidney Diseases, MD) for kindly providing Smad3 deficient (Smad3$^{-/-}$) mice, and Dr F. G. Issa, for the critical reading of the manuscript. This study was supported in part by a Grant-in-Aid for Scientific Research by Japan Society for the Promotion of Science and the Japanese Ministry of Health, Labour and Welfare.

Disclosure

None of the authors has any conflict of interest with the subject matter or materials discussed in the manuscript.

References

1 King TE Jr. Clinical advances in the diagnosis and therapy of the interstitial lung diseases. Am J Respir Crit Care Med 2005; **172**:268–79.

2 Luna MA, Bedrossian CW, Lichtiger B, Salem PA. Interstitial pneumonitis associated with bleomycin therapy. Am J Clin Pathol 1972; **58**:501–10.

3 Piguet PF, Collart MA, Grau GE, Kapanci Y, Vassalli P. Tumor necrosis factor/cachectin plays a key role in bleomycin-induced pneumopathy and fibrosis. J Exp Med 1989; **170**:655–63.

4 Nakao A, Fujii M, Matsumura R *et al.* Transient gene transfer and expression of smad7 prevents bleomycin-induced lung fibrosis in mice. J Clin Invest 1999; **104**:5–11.

5 Scheule RK, Perkins RC, Hamilton R, Holian A. Bleomycin stimulation of cytokine secretion by the human alveolar macrophage. Am J Physiol 1992; **262**:386–91.

6 Smith RE, Strieter RE, Phan SH *et al.* Production and function of murine macrophage inflammatory protein-1 alpha in bleomycin-induced lung injury. J Immunol 1994; **153**:4704–12.

7 Zhang K, Gharaee-Kermani M, Jones ML, Warren JS, Phan SH. Lung monocyte chemoattractant protein-1 gene expression in bleomycin-induced pulmonary fibrosis. J Immunol 1994; **153**:4733–41.

8 Hoshino T, Nakamura H, Okamoto M *et al.* Redox-active protein thioredoxin prevents proinflammatory cytokine- or bleomycin-induced lung injury. Am J Respir Crit Care Med 2003; **168**:1075–83.

9 Kuwano K, Hagimoto N, Kawasaki M *et al.* Essential roles of the Fas-Fas ligand pathway in the development of pulmonary fibrosis. J Clin Invest 1999; **104**:13–19.

10 Nakamishi K, Yoshimoto T, Tsustumi H, Okamura H. Interleukin-18 regulates both th1 and th2 response. Annu Rev Immunol 2001; **19**:423–74.
11 Hoshino T, Robert H, Wiltrout RH, Young HA. IL-18 is a potent coinducer of IL-13 in NK and T cells: a new potential role for IL-18 in modulating the immune response. J Immunol 1999; **162**:5070–7.
12 Hoshino T, Yagita H, Ortaldo JR, Wiltrout RH, Young HA. *In vivo* administration of IL-18 can induce IgE production through TH2 cytokine induction and up-regulation of CD40 ligand (CD154) expression on CD4+ T cells. Eur J Immunol 2000; **30**:1998–2006.
13 Hoshino T, Kawase Y, Okamoto M *et al.* IL-18- transgenic mice: *in vivo* evidence of a broad role for IL-18 in modulating immune function. J Immunol 2001; **166**:7014–18.
14 Wild JS, Sigounas A, Sur N *et al.* IFN-gamma-inducing factor (IL-18) increases allergic sensitization, serum IgE, Th2 cytokines, and airway eosinophilia in a mouse model of allergic asthma. J Immunol 2000; **164**:2701–10.
15 Yoshimoto T, Min B, Sugimoto T *et al.* Nonredundant roles for CD1d-restricted natural killer T cells and conventional CD4+ T cells in the induction of immunoglobulin E antibodies in response to interleukin 18 treatment of mice. J Exp Med 2003; **197**:997–1005.
16 Sims JE. IL-1 and IL-18 receptors, and their extended family. Curr Opin Immunol 2002; **14**:117–22.
17 Nakatani-Okuda A, Ueda H, Kashiwamura S *et al.* Protection against bleomycin-induced lung injury by IL-18 in mice. Am J Physiol Lung Cell Mol Physiol 2005; **289**:280–7.
18 Hoshino T, Okamoto M, Sakazaki Y, Kato S, Young HA, Aizawa H. Role of proinflammatory cytokines IL-18 and IL-1β in bleomycin-induced lung injury in humans and mice. Am J Respir Cell Mol Biol 2009; **41**:661–70.
19 Okamoto M, Kato S, Oizumi K *et al.* Interleukin18 (IL-18) in synergy with IL-2 induced lethal lung injury in mice: a potential role for cytokines, chemokines, and natural killer cells in the pathogenesis of interstitial pneumonia. Blood 2002; **99**:1289–98.
20 Chen ES, Greenlee BM, Wills-Karp M, Moller DR. Attenuation of lung inflammation and fibrosis in interferon-gamma-deficient mice after intratracheal bleomycin. Am J Respir Cell Mol Biol 2001; **24**:545–55.
21 Yang HZ, Cui B, Liu HZ *et al.* Targeting TLR2 attenuates pulmonary inflammation and fibrosis by reversion of suppressive immune microenvironment. J Immunol 2009; **182**:692–702.
22 Suzuki T, Chow CW, Downey GP. Role of innate cells and their products in lung immunopathology. Int J Biochem Cell Biol 2008; **40**:1348–61.
23 Kakizaki T, Kohno M, Watanabe M *et al.* Exacerbation of bleomycin-induced injury and fibrosis by pneumonectomy in the residual lung of mice. J Surg Res 2009; **154**:336–44.
24 Li MO, Wan YY, Sanjabi S, Robertson AK, Flavell RA. Transforming growth factor-β regulation of immune responses. Ann Rev Immunol 2006; **24**:99–146.
25 Bonniaud P, Kolb M, Galt T *et al.* Smad3 null mice develop airspace enlargement and are resistant to TGF-β-mediated pulmonary fibrosis. J Immunol 2004; **173**:2099–108.
26 Higashiyama H, Yoshimoto D, Okamoto Y, Kikkawa H, Asano S, Kinoshita S. Receptor-activated Smad localization in bleomycin-induced pulmonary fibrosis. J Clin Pathol 2007; **60**:283–9.
27 Venlatesan N, Pini L, Ludwig MS. Changes in Smad expression and subcellular localization in bleomycin-induced pulmonary fibrosis. Am J Physiol Lung Cell Mol Physiol 2004; **287**:L1342–7.
28 Zhao Y, Geverd DA. Regulation of Smad3 expression in bleomycin-induced pulmonary fibrosis: a negative feedback loop of TGF-β signaling. Biochem Biophys Res Commun 2002; **294**:319–23.
29 Zhao J, Shi W, Wang YL *et al.* Smad3 deficiency attenuates bleomycin-induced pulmonary fibrosis in mice. Am J Physiol Lung Cell Mol Physiol 2002; **282**:L585–93.
30 Laping NJ, Grygielko E, Mathur A *et al.* Inhibition of transforming growth factor (TGF)-β1-induced extracellular matrix with a novel inhibitor of the TGF-β type I receptor kinase activity: SB-431542. Mol Pharmacol 2002; **62**:58–64.
31 Inman GJ, Nicolás FJ, Callahan JF *et al.* SB-431542 is a potent and specific inhibitor of transforming growth factor-β superfamily type I activin receptor-like kinase (ALK) receptors ALK4, ALK5, and ALK7. Mol Pharmacol 2002; **62**:65–74.
32 Matsuyama S, Iwadate M, Kondo M *et al.* SB-431542 and Gleevec inhibit transforming growth factor-β-induced proliferation of human osteosarcoma cells. Cancer Res 2003; **63**:7791–8.
33 Higashiyama H, Yoshimoto D, Kaise T *et al.* Inhibition of activin receptor-like kinase 5 attenuates bleomycin-induced pulmonary fibrosis. Exp Mol Pathol 2007; **83**:39–46.
34 Yang X, Letterio JJ, Lechleider RJ *et al.* Targeted disruption of SMAD3 results in impaired mucosal immunity and diminished T cell responsiveness to TGF-beta. EMBO J 1999; **18**:1280–91.
35 Li S, Kishihara K, Akashi N *et al.* Vδ1$^+$ T cells are crucial for repertoire formation of γδ T cells in the lung. Biochem Biophys Res Commun 2008; **365**:246–51.
36 Batram U, Speer CP. The role of transforming growth factor beta in lung development and disease. Chest 2004; **125**:754–65.
37 Bellone G, Aste-Amezage M, Trinchieri G, Rodeck U. Regulation of NK cell functions by TGF-β1. J Immunol 1995; **155**:1066–73.

Clinical & Experimental Immunology
The Journal of Translational Immunology

Clinical and Experimental Immunology ORIGINAL ARTICLE doi:10.1111/j.1365-2249.2009.04031.x

Laser microdissection-based analysis of cytokine balance in the kidneys of patients with lupus nephritis

Y. Wang,* S. Ito,* Y. Chino,* D. Goto,* I. Matsumoto,* H. Murata,* A. Tsutsumi,* T. Hayashi,* K. Uchida,† J. Usui,‡ K. Yamagata‡ and T. Sumida*

Division of Clinical Immunology, Doctoral Program in Clinical Sciences, †Molecular and Biological Oncology, and ‡Division of Pathophysiology of Renal Diseases, Graduate School of Comprehensive Human Sciences, University of Tsukuba, Tennodai, Tsukuba, Japan

Accepted for publication 28 August 2009
Correspondence: S. Ito, Division of Clinical Immunology, Doctoral Program in Clinical Sciences, Graduate School of Comprehensive Human Sciences, University of Tsukuba, 1-1-1 Tennodai, Tsukuba 305-8575, Japan.
E-mail: s-ito@md.tsukuba.ac.jp

Summary

To determine the cytokine balance in patients with lupus nephritis (LN), we analysed kidney-infiltrating T cells. Renal biopsy samples from 15 systemic lupus erythematosus (SLE) patients were used. In accordance with the classification of International Society of Nephrology/Renal Pathology Society, they were categorized into Class III, Class III+V (Class III-predominant group, $n = 4$), Class IV, Class IV+V (Class IV-predominant group, $n = 7$) and Class V ($n = 4$) groups. The single-cell samples of both the glomelular and interstitial infiltrating cells were captured by laser-microdissection. The glomerular and interstitial infiltrating T cells produced interleukin (IL)-2, IL-4, IL-10, IL-13 and IL-17 cytokines in the Class III-predominant, Class IV-predominant and Class V groups. Interferon-gamma was detected only in the glomeruli of the Class III-predominant and Class V group samples. The expression level of IL-17 was correlated closely with clinical parameters such as haematuria, blood urea nitrogen level, SLE Disease Activity Index scores in both glomeruli and interstitium, urine protein level in glomeruli and serum creatinine and creatinine clearance levels in interstitium. This suggests that the glomerular infiltrating T cells might act as T helper type 1 (Th1), Th2 and Th17 cells while the interstitial infiltrating T cells, act as Th2 and Th17 cells in the Class III-predominant and Class V groups. In contrast, both the glomerular and interstitial infiltrating T cells might act as Th2 and Th17 cells in the Class IV-predominant group. The cytokine balances may be dependent upon the classification of renal pathology, and IL-17 might play a critical role in SLE development.

Keywords: laser-microdissection, lupus nephritis, SLEDAI, Th17

Introduction

Systemic lupus erythematosus (SLE) is a multi-system autoimmune disease characterized by various clinical manifestations. T cell-derived cytokine production plays a determinant role in SLE development. Previous studies have reported that an imbalance in cytokine production between T helper type 1 (Th1) and Th2 T cells (predominance of Th2 cytokine) in the peripheral blood of SLE patients is associated with the pathogenesis of the disease [1–3]. In contrast, Akahoshi *et al.* [4] demonstrated that a substantial predominance of Th1-type response took place in the peripheral blood samples of lupus nephritis (LN) patients categorized in WHO Class IV. Not only T cells in the peripheral blood, but also the balance in cytokine production between Th1 and Th2 cells in the kidney has drawn a great deal of attention. Masutani *et al.* [5] analysed the expression levels of interferon (IFN)-γ and interleukin (IL)-4 on intrarenal T cells as well as those in the peripheral blood samples from SLE patients with diffuse proliferative LN by immunohistochemistry, demonstrating the predominance of Th1 type response. They suggested that the Th1 : Th2 ratio in the peripheral blood might directly reflect the local histopathological findings. However, Murata *et al.* [6] indicated that the kidney-infiltrating T cells could produce Th2 type cytokines such as IL-4 and IL-10 through reverse transcription–polymerase chain reaction (RT–PCR), and made an assumption that this discrepancy might arise from a difference in sensitivity between the methods used in detection of cytokines. The expression level of IL-13, one of the Th2 type cytokines, was reported to be higher in the serum from the rheumatoid arthritis (RA), SLE, Sjögren's syndrome and

systemic sclerosis patient groups than that in the normal healthy control group [7]. Morimoto *et al.* [8] also showed elevated expression level of IL-13 in SLE patients. Recently, it has been reported that naive murine $CD4^+$ T helper cells can be induced to differentiate into Th1, Th2, Th17 and regulatory phenotypes [9]. IL-17 is a proinflammatory cytokine, as possibly known from the pathological conditions of various inflammatory diseases in both humans and mice [9]. We have reported previously that both IL-13 and IL-17 were produced in the murine LN (MRL/lpr mice) cells; however, we did not analyse them at a single-cell level [10]. The laser microdissection (LMD) technique has been adopted recently to obtain tissue samples exclusively from specific regions of interest. This new technique has been used successfully in various fields, including oncology [11], endocrinology [12], gastroenterology [13], rheumatology [14–16] and nephrology [10,17–19]. With this technique, attempts to analyse single-cell gene expression were made [13,16,20]. In our study, we analysed the single-cell expression levels of cytokines, including IL-13 and IL-17, by infiltrating T cells in the kidneys of LN patients.

Patients and methods

Renal biopsy samples were obtained from 15 SLE patients, two minor glomerular abnormalities (MGA) patients (female, 16 years old; male, 14 years old) and one minimal change nephrotic syndrome (MCNS) patient (male, 14 years old), and used in our experiments. In accordance with the classification criteria defined by International Society of Nephrology/Renal Pathology Society (ISN/RPS) [21,22], renal pathologies were diagnosed as: Class III, three cases; Class III+V, one case; Class IV, two cases; Class IV+V, five cases; and Class V, four cases. To ensure consistency with the World Health Organization (WHO) classification criteria, a further membranous lesion (Class V) may be added to Class III or Class IV in ISN/RPS. They were categorized as Class III-predominant group (Class III-predominant group included patients with both Class III and Class III+V, $n = 4$) and Class IV-predominant group (including patients with both Class IV and Class IV+V, $n = 7$). The patients, who had underwent renal biopsy before 2004, had already been classified in accordance with the WHO classification criteria [23] at the time of biopsy, but in this study were re-evaluated by nephrologists in accordance with the ISN/RPS classification criteria. The SLE Disease Activity Index (SLEDAI) scores [24], histological activity index (AI) and chronicity index (CI) scores [25] at renal biopsy are shown as Table 1. This study was approved by the ethical committee of Tsukuba University Hospital (no. 392). Prior written consent was given by the patients.

Immunohistological examinations

Five-μm-thick sections were obtained from the renal biopsy specimens of the SLE patients. Immunohistochemical

Table 1. Clinical characteristics of patient and positivity of dissected T cells.

No.	Age	Sex	Classification	Pre-s	UP (g/day)	Haematuria (RBC/HPF)	Urinary cast	Pyuria	BUN (mg/dl)	Cr (mg/dl)	Ccr (ml/min)	ADNA (U/ml)	CH50 (U/ml)	SLEDAI	TCR-cβ/ β-actin (%)	AI	CI
1	45	F	III (A)	No	5·0	10–19	+	−	10·1	0·54	92·1	> 300	4·8	17	18/28 (64·3%)	5	2
2	52	F	III (C)	Yes	0·46	1–4	−	−	20·7	1·01	38·9	< 2	40·2	0	15/34 (44·1%)	1	8
3	52	F	III (A) + V	No	0·3	1–4	−	−	10·0	0·57	84·0	64·7	18·2	9	18/26 (69·2%)	0	3
4	29	F	IV-G (A/C)	No	8·0	56	+	+	31·1	1·10	48·1	100·0	12·0	21	28/36 (77·8%)	16	3
5	25	F	IV-G (A/C)	Yes	5·0	5–9	+	−	15·0	0·60	93·0	> 300	2·1	19	18/25 (72·0%)	11	3
6	58	F	IV-S(A/C)+V	No	6·1	1–4	+	−	10·0	0·56	159·0	45	24·5	16	53/67 (79·1%)	12	4
7	59	F	IV-G(A/C)+V	No	2·3	1–4	−	+	26·1	0·95	51·5	64·7	18·2	9	19/28 (67·9%)	5	2
8	55	F	IV-G (A) + V	No	0·8	1–4	−	−	13·1	0·49	100·0	94·6	7·4	13	14/27 (51·9%)	10	0
9	18	F	IV-S (A) + V	Yes	0·46	1–4	−	−	12·3	0·48	108·5	58·1	9·5	18	22/31 (70·1%)	6	3
10	28	F	V	No	7·7	0–1	−	−	13·8	0·70	96·7	16·7	41·6	5	18/26 (69·2%)	1	2
11	39	F	V	Yes	5·3	0–1	−	−	12·4	0·51	138·1	5·4	50·7	4	22/32 (68·8%)	0	2
12	26	F	V	Yes	2·1	5–9	−	−	13·5	0·60	95·4	23·1	42·9	19	46/62 (74·2%)	0	0
13	22	M	IV-G(A/C)+V	Yes	4·15	30–50	+	−	16·0	0·90	110·8	< 5·0	20·5	10	7/20 (35·0%)	8	6
14	38	F	III (A/C)	No	0·85	1–4	+	−	18·7	0·62	141·7	> 300	23·2	13	18/31 (58·1%)	6	4
15	60	F	V	No	0·49	20–99	−	−	16·6	0·73	99·6	20·3	54·0	22	27/40 (67·5%)	0	3

S: segmental; G: global; A: active; C: chronic; Pre-s: pretreatment with steroid; UP: urine protein; RBC/HPF: red blood cell/high power field; BUN: blood urea nitrogen; Cr: serum creatinine; Ccr: creatinine clearance; Anti-ds: anti-double-stranded DNA; CH50: 50% haemolytic unit of complement serum; SLEDAI: systemic lupus erythematosus Disease Activity Index; AI: activity index score; CI: chronicity index score.

staining was performed by the avidin–biotin complex technique. Primary antibodies used included murine anti-human IFN-γ (Santa Cruz Biotechnology, Santa Cruz, CA, USA); anti-IL-4, 10 (Research & Diagnostics Systems, Minneapolis, MN, USA); and polyclonal rabbit anti-human IL-17 and IL-13 (Santa Cruz Biotechnology). Staining was performed on the sections using normal murine IgG or rabbit immunoglobulin (Ig)G, a primary antibody, as a negative control. We also performed staining on sections of the renal biopsy samples of MGA and MCNS patients using anti-human IL-17 as the control.

Tissue sampling by laser microdissection

Frozen sections (10 μm thick) from the renal biopsy specimens of the SLE patients were stained with 0·05% toluidine blue solution (pH 7·0) (Wako Pure Chemical Industries, Osaka, Japan) and the individual single cells infiltrating into glomeruli and interstitiums were selected and dissected with laser-microdissection system (AS-LMD; Leica Microsystems Japan, Tokyo, Japan) (Fig. 2A).

RNA extraction and nested RT–PCR

Total RNA was extracted from the LMD samples by the Isogen method (Nippon Gene, Tokyo, Japan) according to the manufacturer's instructions. First-strand cDNA was prepared from total RNA using the ThermoScript RT–PCR System (Invitrogen Life Technologies, Carlsbad, CA, USA) and amplified with primers specific to β-actin, T cell receptor β chain (TCR-Cβ), IL-2, IL-4, IL-10, IL-13, IL-17 and IFN-γ for nested RT–PCR (Table 2).

Statistical analysis

All data were expressed as mean ± standard error of the mean. Statistically significant differences between groups were determined using the Mann–Whitney *U*-test. A simple linear regression analysis was used to evaluate the correlation between the two parameters. The statistical significance was defined as $P < 0.05$.

Results

Detection of T cells in glomeruli and interstitium

Stained IL-4, IL-10 and IL-13 were observed in the glomerular and interstitial areas of the specimens from the SLE patients of the Class III-predominant, IV-predominant and Class V groups, especially in the latter area of the Class IV-predominant group (Fig. 1A) (the immunohistochemical data for the Class III-predominant and Class V groups are not shown). Many IL-4 cells were observed predominantly, mainly in the glomerular and interstitial cells, especially in intraglomerular infiltrating cells, in the Class IV-predominant group, while there were only a few IL-4-positive cells in the tubular epithelial cells (TEC) (Fig. 1Aa, b). IL-10- and IL-13-positive cells were observed prominently in the glomerular and interstitial infiltrating cells (Fig. 1Ac–f). Some stained IL-10-positive cells were observed in TEC (Fig. 1Ac, d). IL-17-positive cells were observed mainly in the glomerular and interstitial infiltrating cells and TECs, especially in intraglomerular cells of the Class IV-predominant group (Fig. 1Ag, h). Almost no IL-17-positive cells were observed in the glomeruli of the Class III-predominant (Fig. 1Ba) and Class V group (not shown) samples. However, IFN-γ cells were not observed in all the specimens (Fig. 1Bb) (the immunohistochemical data for the Class III-predominant groups are shown). Normal rabbit IgG was used as a negative control (Fig. 1Bc). IL-17-positive cells were not observed in all the specimens from the MGA and MCNS patients (Fig. 1C). This demonstrates that IL-17 may be produced preferentially in SLE patients.

Analysis of gene expression by laser microdissection and nested RT–PCR

Of 622 glomerular and interstitial infiltrating cells, 513 (82·5%) were β-actin-positive, among which 343 (66·7%) were TCR-Cβ-positive; these 343 cells were deemed to be T cells and used for cytokine analysis (Table 1). The number of positive samples for each cytokine/ TCR-Cβ$^+$ cells was expressed as a percentage.

The glomerular and interstitial infiltrating T cells produced IL-2, IL-4, IL-10, IL-13 and IL-17 cytokines in the Class III-predominant, Class IV-predominant and Class V groups. The positivity of cytokines is shown in Table 3 and Fig. 2B. The percentages of positive IL-4, IL-10 and IL-13 samples were more than 70%, 67% and 41%, respectively, in all the groups. The expression levels of IL-2 were low in each of the predominant groups. IFN-γ was detected only in the glomeruli of the Class III-predominant and Class V groups (32·3 ± 12·9% and 24·0 ± 10·0%, $P < 0.05$) (Table 3 and Fig. 2B). In the glomerular lesions, the percentage of positive IL-17 samples was 64·7 ± 10·1% and 70·7 ± 6·0% in the Class IV-predominant and V groups, while it was significantly greater than in the Class III-predominant group (44·7 ± 5·9%, $P < 0.05$) (Fig. 2Bb). In the interstitial lesions, the positivity of IL-17 (48·0 ± 4·2%) was also significantly lower in the Class III-predominant groups than that in the Class IV-predominant group (69·1 ± 8·9%, $P < 0.05$) (Fig. 2Bc).

Correlation between the expression levels of cytokines and clinical parameters in SLE patients

We analysed the correlation between the expression levels of Th1 (IL-2), Th2 (IL-4, IL-10, and IL-13) and Th17 (IL-17)

Table 2. Oligonucleotide primer sequences.

PCR products		Oligonucleotide sequence	Product size (bp)	RT–PCR cycles
β-actin				
First PCR	5′ sense	GGCATCCTCACCCTGAAGTA	496	25
	3′ anti-sense	CCATCTCTTGCTCGAAGTCC		
Nested PCR	5′ sense	AAATCTGGCACCACACCTTC	262	25
	3′ anti-sense	AGGGCATACCCCTCGTAGAT		
TCR-Cβ				
First PCR	5′ sense	ACATAAGGAAGGCTGCATGG	249	30
	3′ anti-sense	CGTTTTGATCATGGTGTGTGG		
Nested PCR	5′ sense	ATCAGGTGTGTGGGACTTTG	217	30
	3′ anti-sense	GACTCAGGACAGTGACATCA		
IFN-γ				
First PCR	5′ sense	TCTGCATCGTTTTGGGTTCTC	346	25
	3′ anti-sense	TCAGCTTTTCGAAGTCATCTC		
Nested PCR	5′ sense	TGTTACTGCCAGGACCCATAT	242	30
	3′ anti-sense	ACTCTTTTGGATGCTCTGGTC		
IL-2				
First PCR	5′ sense	ACTACCAGGATGCTCACATT	267	25
	3′ anti-sense	AAGGTAATCCATCTGTTCAGA		
Nested PCR	5′ sense	GCCACAGAACTGAAACATCTT	201	30
	3′ anti-sense	TTCTACAATGGTTGCTGTCTC		
IL-4				
First PCR	5′ sense	CTTCCCCCTCTGTTCTTCCT	318	25
	3′ anti-sense	TTCCTGTCGAGCCGTTTCAG		
Nested PCR	5′ sense	CTAGCATGTGCCGGCAACTTT	273	25
	3′ anti-sense	TCGGATCAGCTGCTTGTGCCT		
IL-10				
First PCR	5′ sense	ACAGCTCAGCACTGCTCTGT	327	30
	3′ anti-sense	AGTTCACATGCGCCTTGATG		
Nested PCR	5′ sense	CCCAGTCTGAGAACAGCTGCAA	210	30
	3′ anti-sense	CTGGGTCTTGGTTCTCAGCTT		
IL-13				
First PCR	5′ sense	CTATGCATCCGCTCCTCAAT	391	30
	3′ anti-sense	TTTACAAACTGGGCCACCTC		
Nested PCR	5′ sense	ATTGCTCTCACTTGCCTTGG	229	25
	3′ anti-sense	TCCTGTGGGTCTTCTCGATC		
IL-17				
First PCR	5′ sense	CTTCACCCTGTGGAACGAAT	262	30
	3′ anti-sense	CGGAATTGGTTCTGGAGTGT		
Nested PCR	5′ sense	GAGCACATGCACCACATACC	170	25
	3′ anti-sense	AGGAAACAGTCGCGGAGTGT		

RT–PCR: reverse transcription polymerase chain reaction; TCR-Cβ: T cell receptor β chain; IL: interleukin; IFN-γ: interferon-gamma; bp: base pairs.

Table 3. Positivity of cytokines in glomeruli and interstitiums (%).

	Glomeruli			Interstitiums		
	Class III predominant	Class IV predominant	Class V	Class III predominant	Class IV predominant	Class V
IL-2	19·7 ± 10·3	23·7 ± 20·3	44·6 ± 12·8	25·6 ± 10·5	2·8 ± 21·7	27·9 ± 12·3
IFN-γ	32·3 ± 12·9	n.d.	24·0 ± 10·0	3·1 ± 3·8	n.d.	1·3 ± 1·6
IL-4	88·6 ± 9·1	80·4 ± 13·5	85·7 ± 7·1	90·6 ± 7·5	84·6 ± 13·5	70·9 ± 16·7
IL-10	67·2 ± 5·1	67·7 ± 14·3	70·0 ± 10·3	70·5 ± 6·4	84·3 ± 6·5	79·8 ± 8·1
IL-13	60·6 ± 15·7	47·6 ± 20·5	62·3 ± 9·3	52·0 ± 9·2	41·5 ± 13·4	62·3 ± 7·6
IL-17	44·7 ± 5·9	64·7 ± 10·1*	70·7 ± 6·0*	48·0 ± 4·2	69·1 ± 8·9*	62·6 ± 12·3

*$P < 0.05$ *versus* Class III-predominant groups. Results are expressed as mean ± standard error of the mean. Statistical significance was determined using the Mann–Whitney *U*-test. IL; interleukin; IFN-γ: interferon-gamma; n.d.: not determined.

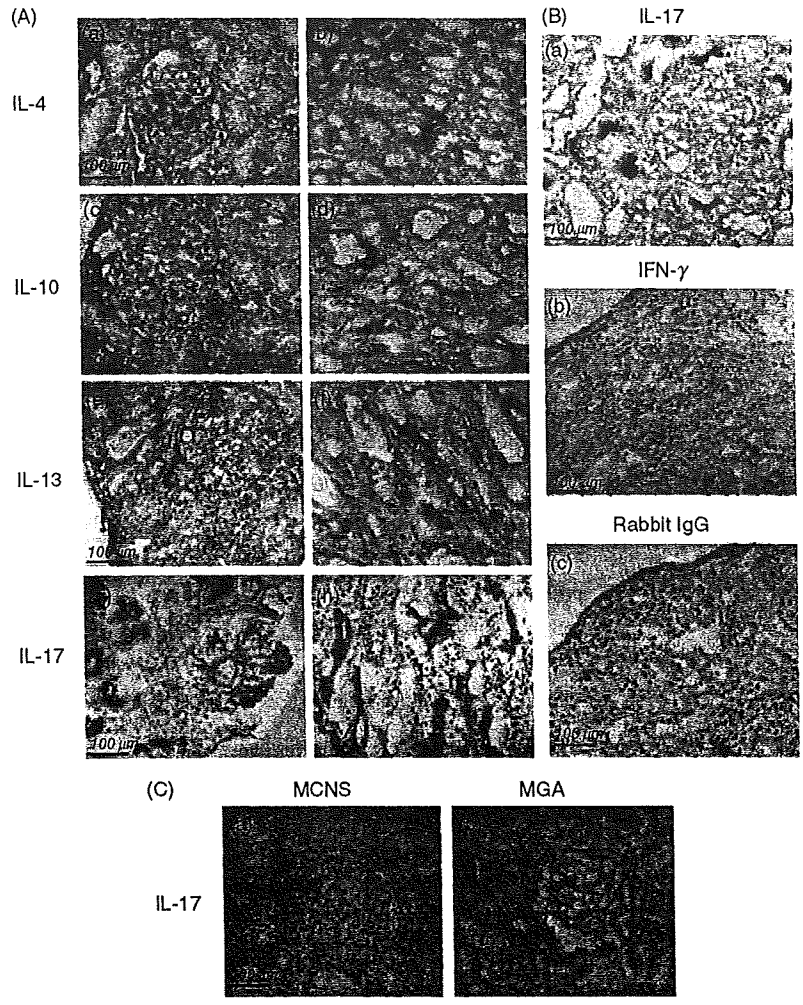

Fig. 1. Detection of T cells in glomeruli and interstitium. (A) Stained interleukin (IL)-4, IL-10, IL-13 and IL-17 were observed in glomeruli and interstitium areas of the Class IV-predominant groups. Many IL-4 cells are observed prominently, mainly in the cells infiltrating into the glomeruli and interstitium areas, especially in intraglomerular infiltrating cells. There are only a few IL-4 cells in the tubular epithelial cells (TEC) (a, b). IL-10 and IL-13 cells are observed prominently in some of the cells infiltrating into the glomeruli and interstitium areas (c–f). Some stained IL-10 cells were observed in TEC (d). Many IL-17 cells are observed prominently, mainly in the cells infiltrating into the glomeruli, interstitium areas and TEC (g, h), especially in intraglomerular cells and TEC (g) (original magnification × 100 in a–h). (B) In the Class III-predominant group, some stained IL-17 cells were observed in TEC but almost no IL-17-positive cells were observed in glomeruli (a). Interferon (IFN)-γ cells were not observed in all the specimens (b). Normal rabbit immunoglobulin (Ig)G was stained as negative control (c) (original magnification × 100). (C) IL-17-positive cells were not observed in all the specimens of minor glomerular abnormalities (MGA) and minimal change nephrotic syndrome (MCNS) (a, b) (original magnification × 100).

cytokines and clinical parameters in SLE patients, such as the urine protein (UP) level, haematuria, blood urea nitrogen (BUN) level, serum creatinine (Cr) level, creatinine clearance (Ccr), 50% haemolytic unit of complement serum (CH50), anti-double-strand DNA (anti-ds DNA) antibodies, SLEDAI scores, histological AI and CI (Table 4). Good and significant correlation data are shown in Fig. 3.

Correlation between Th1 cytokine and clinical parameters. In glomeruli, as known from the tendency of the point distribution on the charts, the parameters, BUN ($r = 0{\cdot}27$), Ccr ($r = 0{\cdot}31$), AI ($r = -0{\cdot}28$), CI ($r = 0{\cdot}39$) and SLEDAI ($r = -0{\cdot}21$) ($P < 0{\cdot}05$) showed a weak correlation with the expression level of IL-2 (Table 4). The expression level of IL-2 showed a good correlation with anti-ds DNA antibodies ($r = -0{\cdot}53$, Fig. 3Aa) and a significant correlation with CH50 ($r = 0{\cdot}80$, $P < 0{\cdot}001$, Fig. 3Ab). In the interstitium, haematuria ($r = -0{\cdot}36$), BUN ($r = -0{\cdot}24$), Cr ($r = -0{\cdot}35$) and CH50 ($r = 0{\cdot}37$) showed a weak correlation with the expression level of IL-2 (Table 4); Ccr ($r = 0{\cdot}63$) and CI ($r = 0{\cdot}404$) showed a good correlation with the expression level of IL-2 (Fig. 3Ac, d).

Correlation between Th2 and clinical parameters. In the glomeruli, haematuria ($r = 0{\cdot}44$), BUN ($r = -0{\cdot}44$), Cr ($r = -0{\cdot}41$) and CI ($r = -0{\cdot}59$) showed a good correlation with the expression level of IL-4 (Fig. 3Ba–d); SLEDAI ($r = -0{\cdot}36$) and AI ($r = -26$) showed a weak correlation with IL-4 (Table 4). The expression level of IL-10 showed a weak correlation with haematuria ($r = -0{\cdot}23$), BUN ($r = -0{\cdot}39$), Ccr ($r = 0{\cdot}27$), CI ($r = 0{\cdot}28$) and CH50 ($r = 0{\cdot}31$). However, there was almost no finding that showed any correlation with the expression level of IL-13 except for BUN ($r = -0{\cdot}21$), AI ($r = -0{\cdot}32$) and CH50 (Table 4).

In the interstitiums, there was a weak correlation in the expression level of IL-4 with haematuria ($r = 0{\cdot}24$), CH50 ($r = -0{\cdot}34$), AI ($r = 0{\cdot}22$), CI ($r = -0{\cdot}33$) and anti-ds DNA antibodies ($r = 0{\cdot}28$) (Table 4). IL-10 showed a good correlation with UP ($r = 0{\cdot}59$) (Fig. 3Be) and a weak correlation with SLEDAI ($r = -0{\cdot}26$) (Table 4). The percentage of IL-13

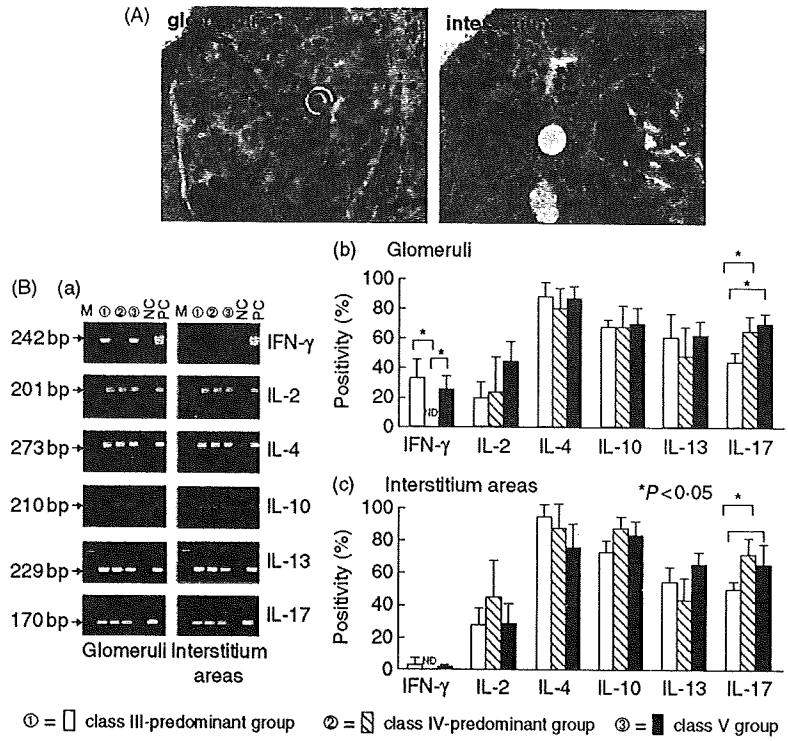

Fig. 2. (A) Targeted infiltrating cells selected and cut by laser microdissection (LMD). The glomeruli and interstitium areas of a single infiltrating cell (black arrows) were selected and dissected with a laser microbeam one by one. (B) Analysis of cytokine gene expression in lesions. (a) Detection of cytokines in the lesions of the renal biopsy specimens from the patients by nested polymerase chain reaction (PCR). Specific expression of interferon (IFN)-γ, interleukin (IL)-2, IL-4, IL-10, IL-13 and IL-17 were identified in the lesions of the glomeruli and interstitium areas from the renal biopsy specimens of the patients in the Class III-predominant groups ($n=4$), Class IV-predominant groups ($n=7$) and Class V groups ($n=4$). M: molecular size marker; NC: negative control; PC: positive control cDNA clone. (b) Expression of IFN-γ, IL-2, IL-4, IL-10, IL-13 and IL-17 mRNAs in the glomeruli areas of the Class III-predominant (white bars), Class IV-predominant (hatched bars) and Class V (black bars) groups was analysed by nested reverse transcription–polymerase chain reaction (RT–PCR). (c) Expression of IFN-γ, IL-2, IL-4, IL-10, IL-13 and IL-17 mRNAs in the interstitium areas of the Class III-predominant (white bars), Class IV-predominant (hatched bars) and Class V (black bars) groups was analysed by nested RT–PCR (n.d. = not determined). The number of positive samples is shown as a percentage. Error bars represent ± standard error. $P < 0·05$, by Mann–Whitney *U*-test.

samples showed a weak correlation with UP ($r=-0·35$), haematuria ($r=-0·31$) and Ccr ($r=0·37$) (Table 4), and a good correlation with BUN ($r=-0·68$), Cr ($r=-0·49$), CH50 ($r=0·48$), AI ($r=-0·54$) and anti-ds DNA antibodies ($r=-0·43$) (Fig. 3C).

Correlation between Th17 and clinical parameters. In the glomeruli, UP ($r=0·33$), AI ($r=0·26$), CI ($r=-0·34$) and BUN ($r=0·26$) showed a weak correlation with the expression level of IL-17 (Table 4). Haematuria ($r=0·54$) and SLEDAI ($r=0·54$) showed a significantly positive correlation with the expression level of IL-17 (Fig. 3Da, b). In the interstitiums, the positive IL-17 samples showed a weak correlation with BUN ($r=0·37$), Cr ($r=0·38$), AI ($r=0·29$), CI ($r=-0·27$) and Ccr ($r=-0·36$) (Table 4), and a good correlation with haematuria ($r=0·47$) and SLEDAI ($r=0·54$) (Fig. 3Da, b). In particular, focusing upon patients whose SLEDAI scores are more than 10, there is a highly significant correlation between SLEDAI scores and the expression levels of IL-17 both in the glomeruli ($r=0·81$, $P<0·05$) and the interstitiums ($r=0·87$, $P<0·001$) (Fig. 3Dc).

Discussion

A cytokine balance of T helper cells in the kidneys of LN patients has drawn a great deal of attention [5,6]. We analysed the single-cell cytokine profile of the samples from the LN patients, including IL-13 and IL-17, by LMD. We observed the predominance of the Th2 cytokine both in the glomeruli and the interstitiums; this corresponds to the results of the study using whole kidneys by Murata *et al.* [6]. However, IFN-γ was observed only in the glomeruli of the ISN/RPS Class III-predominant and Class V groups. Chan *et al.* [19] reported that up-regulation of IFN-γ, IL-2 and T-bet (the Th1 transcription factor) was observed and no difference was observed in glomerular expression level of any

Table 4. Correlation between the levels of cytokines and clinical parameters.

				Glomeruli						
	SLEDAI	CH50	ADNA	haematuria	Cr	BUN	AI	CI	UP	Ccr
IL-2	−0.214*	0.795***	−0.53**	0.363*	0.114	−0.27*	−0.279*	0.387*	0.045	0.31*
	0.049	0.002	0.018	0.046	0.242	0.047	0.047	0.045	0.435	0.047
IL-4	−0.361*	−0.065	0.016	−0.437**	−0.405*	−0.441**	−0.262*	−0.591**	−0.115	−0.095
	0.046	0.592	0.47	0.042	0.041	0.044	−0.048	0.01	0.34	0.367
IL-10	−0.156	0.308*	0.194	−0.231*	0.019	−0.391*	−0.091	0.282*	0.187	0.265*
	0.268	0.047	0.143	0.048	0.472	0.045	0.626	0.046	0.049	0.047
IL-13	0.001	0.342*	−0.192	0.162	0.023	−0.213*	−0.319*	0.022	0.038	0.127
	0.499	0.047	0.045	0.146	0.467	0.049	0.047	0.531	0.445	0.325
IL-17	0.541**	0.123	−0.157	0.543**	0.029	0.264*	0.227*	−0.341*	0.333*	0.007
	0.017	0.33	0.278	0.018	0.458	0.049	0.049	0.046	0.047	0.488
				Interstitium						
	SLEDAI	CH50	ADNA	haematuria	Cr	BUN	AI	CI	UP	Ccr
IL-2	−0.125	0.37*	−0.175	−0.362*	−0.348*	−0.24*	0.173	0.404**	0.154	0.63**
	0.327	0.045	0.265	0.046	0.046	0.048	0.268	0.037	0.29	0.016
IL-4	0.178	−0.34*	0.279*	−0.24*	−0.168	0.07	0.221*	−0.333*	−0.062	−0.084
	0.262	0.046	0.047	0.044	0.273	0.401	0.048	0.046	0.413	0.381
IL-10	−0.26*	−0.116	−0.02	−0.094	0.207	0.037	0.195	0.061	0.586**	−0.058
	0.047	0.339	0.471	0.369	0.059	0.447	0.091	0.414	0.012	0.418
IL-13	0.058	0.483**	−0.436**	0.31*	−0.486**	−0.675**	−0.541**	−0.117	−0.35*	0.371*
	0.418	0.033	0.025	0.047	0.039	0.002	0.018	0.338	0.047	0.046
IL-17	0.544**	−0.134	0.476*	0.471*	0.379*	0.374*	0.294*	−0.273*	−0.028	−0.364*
	0.018	0.316	0.036	0.038	0.045	0.042	0.047	0.048	0.459	0.047

Correlation between clinical parameters and cytokines was assessed by using the Pearson correlation coefficient test (r-value showed in up, *r = 0·2–0·4, weak correlation; **r = 0·4–0·7, good correlation; ***r = 0·7–0·9, significant correlation. P-value showed in down). UP: urine protein; RBC/HPF: red blood cell/high power field; BUN: blood urea nitrogen; Cr: serum creatinine; Ccr: creatinine clearance; ADNA: anti-double-stranded DNA; CH50: 50% haemolytic unit of complement serum; SLEDAI: systemic lupus erythematosus Disease Activity Index; AI: activity index score; CI: chronicity index; IL: interleukin.

target genes between the WHO Classes. However, as they reported, they did not analyse at a single-cell level; therefore, they could not identify the cellular origin of the detected mRNA, which is likely to be the reason for the discrepancy between their results and our results. Morimoto *et al.* [8] reported that Th2 predominance in the peripheral blood might induce renal lesions, and the co-existence of Th1 and Th2 might cause haemolytic anaemia or pulmonary lesions in SLE patients. Our result demonstrates that Th1 has a role in protecting the kidneys of LN patients; this corresponds to the results of the experiments on the peripheral blood of the SLE patients reported by Morimoto *et al.* Although, conventionally, it was believed that enhanced Th1 cell activation and IFN-γ production might contribute to the development of autoimmune diseases [26,27], certain findings have exploded this general hypothesis. For example, experimental autoimmune nephritis and collagen-induced arthritis (CIA) was exacerbated in mice treated with anti-IFN-γ-neutralizing antibodies and in IFN-γ-deficient or IFN-γ receptor-deficient mice [28]. Haas *et al.* [29] reported that IFN-γ might play a key role in suppressing the development of nephritis in MRL/lpr mice (SLE models).

In addition to the helper T cells classified into Th1 and Th2 types, another helper T cell subset, Th17, has been discovered recently [9]. It has been observed that IL-17 has a proinflammatory role in many inflammatory conditions [9], contributing to the pathogenesis of autoimmune and inflammatory diseases, including SLE [30].

Elevated concentrations of proinflammatory cytokines (IL-18, IL-17, IL-12) and Th2 cytokine (IL-4) in the SLE patients were reported [31]. Dong *et al.* [32] reported that the cultured peripheral blood mononuclear cells (PBMC) of LN patients stimulated by IL-17 produced significantly high levels of IL-6, IgG and anti-ds DNA antibodies. However, IL-17 did not increase them in cultured PBMC of normal controls [32]. Crispin *et al.* [33] have demonstrated that $CD3^+$ $CD4^-CD8^-$ double-negative (DN) T cells from SLE patients produce significant amounts of IL-17 and IFN-γ. Furthermore, $IL\text{-}17^+$ and DN T cells are found in renal biopsy specimens from LN patients. In our study, we have confirmed successfully the production of IL-17 in infiltrating T cells in the kidneys (glomeruli and interstitiums) of the LN patients at a single-cell level. This suggests that IL-17 may play an important role in the LN patients. It was reported

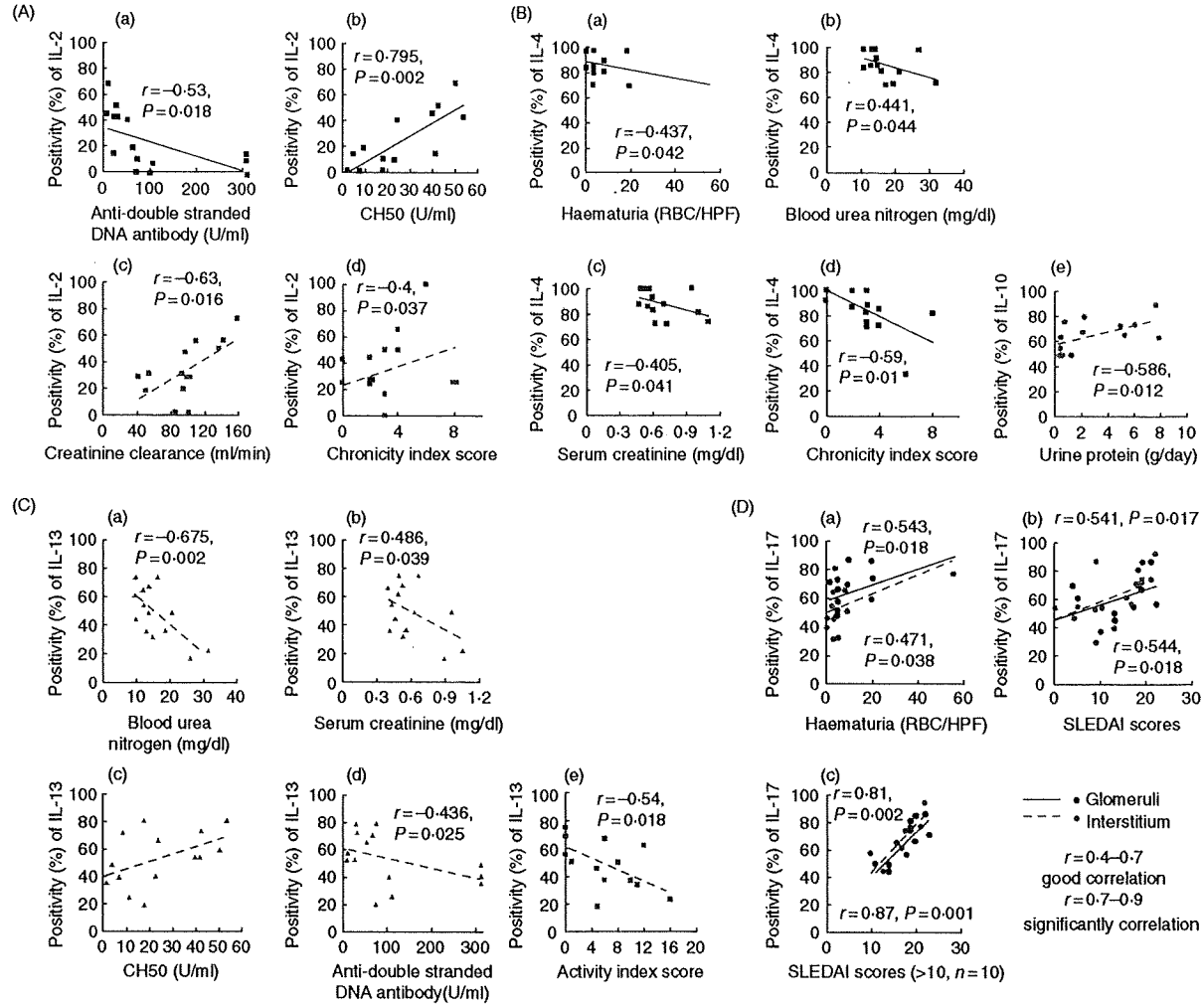

Fig. 3. Correlation between T helper type 1 (Th1), Th2 and Th17 cytokines and clinical and laboratory parameters in systemic lupus erythematosus (SLE). (A) Correlation between the levels of Th1 cytokine interleukin (IL)-2 and anti-double-strand (ds) DNA antibodies (a), 50% haemolytic unit of complement serum (CH50) (b), creatinine clearance (c) and chronicity index score (d) in glomeruli (black full line and points) and interstitium (black dashed line and grey points). (B) Correlation between the levels of Th2 cytokines–IL-4 and haematuria (a), blood urea nitrogen (b), serum creatinine (c) and chronicity index score (d) in glomeruli (black full line and points). Correlation between the levels of IL-10 and urine protein in interstitium (black dashed line and grey points). (C) Correlation between the levels of IL-13 and blood urea nitrogen (a), serum creatinine (b), 50% haemolytic unit of complement serum (CH50) (c), anti-ds DNA antibodies (d) and Activity Index scores (e) in interstitium. (D) Correlation between the levels of Th17 cytokine (IL-17), haematuria (a) and SLE Disease Activity Index (SLEDAI) scores (b) in glomeruli (black full line and points) and interstitium (black dashed line and grey points). Correlation between the level of IL-17 and SLEDAI scores (> 10) in glomeruli and interstitium (c). A simple linear regression analysis was used to evaluate the correlation between the two parameters, $P < 0{\cdot}05$.

that cyclosporine A might inhibit the production of IL-17 in the healthy control and RA patient groups [34]. Cyclosporine A also inhibits IL-15-induced IL-17 production in the $CD4^+$ T cells through down-regulation of PI3K/Akt and nuclear factor-kappa B (NF-κB) [35]. Inhibition of IL-15-induced IL-17 production by tacrolimus was also observed in $CD4^+$ T cells [35]. It may be considered that the inhibition of IL-17 is an important mechanism of the efficacy of these two kinds of calcineurin inhibitors in the steroid-resistant LN patients.

To confirm cytokine production in the kidney by RT–PCR, we conducted immunohistochemical experiments. The production of IL-13 and IL-17 were also observed by immunohistochemistry. Stained IL-17-positive cells were observed not only in the glomeruli or interstitiums, but also in the tubular epitheliums of LN patients (Fig. 1). Crispin *et al.* [33] reported that IL-17-positive cells were found by immunofluorescence mainly in the tubule-interstitial zone, the area where cellular infiltration is mainly found. We made stains for IL-17-positive cells with anti-human IL-17 in

the specimens from MGA and MCNS patients; no IL-17-positive cells were observed (Fig. 1Ca, b). This has demonstrated that IL-17 may be produced preferentially in SLE patients. Matsumura *et al.* also found stained IL-17 in the tubular epitheliums of LN patients by immunohistochemistry (personal communication). Thus, production of IL-17 in the tubules was confirmed by the RT–PCR and LMD methods. We believe that the RT–PCR technique is more sensitive than immunohistochemistry and can be used for quantification of the production of each cytokine.

We analysed the correlation between the expression levels of Th1, Th2 and Th17 cytokines and clinical parameters. We found that the levels of IL-2, IL-4, IL-10, IL-13 and IL-17 have a correlation with some clinical and laboratory parameters (Fig. 3). A negative correlation was found between the level of IL-2 and haematuria, BUN, Cr, anti-ds DNA antibody and SLEDAI, except for Ccr, CH50 and CI. However, the IL-17 level was correlated positively with UP, haematuria, BUN, Cr, AI and SLEDAI, while correlating negatively with CI and Ccr (Fig. 3). These findings indicate that IL-2 and IL-17 play opposite roles in SLE development. It is suggested that IL-2 may play a role in protecting against SLE development, while IL-17 might have a reverse effect. Wong *et al.* [36] showed significant and positive correlations of plasma IL-17 concentrations with SLEDAI scores in the patients without renal disease. Yang *et al.* [37] showed that patients with active SLE (SLEDAI > 6) exhibit an increased proportion of Th17 cells in $CD3^-CD8^-$ T cells from PBMC compared with healthy individuals by flow cytometric analysis, and a significant positive correlation between the percentage of Th17 cells and the SLEDAI score. Doreau *et al.* [38] also found that the serum of patients with SLE had higher concentrations of IL-17 than did the serum of healthy people, and that IL-17 abundance correlated with the disease severity of SLE. In our study, the level of IL-17 correlated positively and significantly with SLEDAI scores both in the glomeruli and the interstitiums. A highly significant correlation was observed between SLEDAI scores and the level of IL-17 in both the glomeruli and the interstitiums of active SLE patients (SLEDAI > 10) (Fig. 3D). We also found that the level of IL-17 has positive correlations with AI and negative correlations with CI in both glomerulus and interstitium, although correlations were weak (Table 4). This suggests that IL-17 may play an important role in the inflammatory process of a renal disease during the acute phase of SLE patients. With few IFN-γ-positive samples, we did not analyse the correlation between IFN-γ and the clinical and laboratory parameters. IFN-γ was observed only in the glomeruli of ISN/RPS Class III-predominant and Class V groups; accordingly, IFN-γ might play a role in protecting against the inflammatory process in LN patients, as with IL-2. The IL-2 level correlatates good positively with CI, suggesting that IL-2 might act during the chronic stage of glomerulonephritis (Fig. 3A and Table 4). Nakae *et al.* [39] found that IL-17 can suppress Th1 cell differentiation in the presence of exogenous IL-12 *in vitro*, and IFN-γ can down-regulate Th17 cell differentiation. Not only IFN-γ but also IL-4 can suppress IL-17 production *in vitro* [40,41]. Chu *et al.* [42] demonstrated further that IFN-γ might regulate susceptibility to CIA through suppression of IL-17, and IFN-γ and IL-4 together had a synergistic effect on suppression of type II collagen (CII)-specific IL-17 production during CII restimulation *in vitro*. This might be the reason why the expression levels of IFN-γ and IL-4 were higher in the ISN/RPS Class III-predominant group than those of other classes, whereas that of IL-17 was lower. Th2 cytokine showed inconsistent results, but it seems likely that IL-13 plays a protective role in lupus nephritis (Fig. 3C, Table 4).

In conclusion, we have shown that the glomerular infiltrating T cells might act as Th1, Th2 and Th17 cells, while the interstitial infiltrating T cells, as Th2 and Th17 cells in the Class III-predominant and Class V groups. In contrast, both the glomerular and interstitial infiltrating T cells might act as Th2 and Th17 cells in the Class IV-predominant group. The cytokine balances may be dependent on the classification of renal pathology and IL-17 might play a critical role in SLE development.

Acknowledgements

This study was supported by the Health and Labour Sciences Research Grants for Research on Intractable Diseases from the Ministry of Health, Labour and Welfare of Japan. We thank medical scientists of Chiba-East National Hospital (Department of Rheumatology, Allergy and Clinical Immunology National Hospital Organization Chiba-East National Hospital) for their helpful suggestions for this study.

Disclosure

None of the authors have any conflict of interest with the subject matter or materials discussed in the manuscript.

References

1 Funauchi M, Ikoma S, Enomoto H, Horiuchi A. Decreased Th-1 like and increased Th-2 like cells in systemic lupus erythematosus. Scand J Rheumatol 1998; 27:219–24.

2 Viallard JF, Pellegrin JL, Ranchin V *et al.* Th1 [IL-2, interferon-gammma (IFN-γ)] and Th2 (IL-10, IL-4) cytokine production by peripheral blood mononuclear cells (PBMC) from patients with systemic lupus erythematosus (SLE). Clin Exp Immunol 1999; 115:189–95.

3 Richaud-Patin Y, Alcocer-Verela J, Llorente L. High levels of TH2 cytokine gene expression in systemic lupus erythematosus. Rev Invest Clin 1995; 47:267–72.

4 Akahoshi M, Nakashima H, Tanaka Y *et al.* Th1/Th2 balance of peripheral T helper cells in systemic lupus erytematosus. Arthritis Rheum 1999; 42:1644–8.

5 Masutani K, Akahoshi M, Tsuruya K *et al.* Predominance of Th1

immune response in diffuse proliferative lupus nephritis. Arthritis Rheum 2001; 44:2097–106.
6 Murata H, Matsumura R, Koyama A *et al.* T cell receptor repertoire of T cells in the kidneys of patients with lupus nephritis. Arthritis Rheum 2002; 46:2141–7.
7 Spadaro A, Rinaldi T, Riccieri V, Taccari E, Valesini G. Interleukin-13 in autoimmune rheumatic diseases: relationship with the autoantibody profile. Clin Exp Rheumatol 2002; 20:213–6.
8 Morimoto S, Tokano Y, Kaneko H, Nozawa K, Amano H, Hashimoto H. The increased interleukin-13 in patients with systemic lupus erythematosus: relations to other Th1-, Th2-related cytokines and clinical findings. Autoimmunity 2001; 34:19–25.
9 Afzari B, Lombardi G, Lechler R, Lord GM. The role of T helper (Th17) and regulatory T cells (Treg) in human organ transplantation and autoimmune disease. Clin Exp Immunol 2007; 148:32–46.
10 Wang Y, Ito S, Sumida T *et al.* Use of laser microdissection in the analysis of renal-infiltrating T cells in MRL/lpr mice. Mod Rheumatol 2008; 18:385–93.
11 Lechner S, Muller-Landner U, Renke B, Scholmerich J, Ruschoff J, Kullmann F. Gene expression pattern of laser microdissected colonic crypts of adenomas with low grade dysplasia. Gut 2003; 52:1148–53.
12 Hong SH, Nah HY, Lee JY, Gye MC, Kim CH, Kim MK. Analysis of estrogen-regulated genes in mouse uterus using cDNA microarray and laser capture microdissection. J Endocrinol 2004; 181:157–67.
13 Shi X, Kleeff J, Zhu ZW *et al.* Gene-expression analysis of single cells-nested polymerase chain reaction after laser microdissection. World J Gastroenterol 2003; 9:1337–41.
14 Judex M, Neuman E, Gay S, Muller-Lander U. Laser-mediated microdissection as a tool for molecular analysis in arthritis. Methods Mol Med 2004; 101:93–105.
15 Hashimoto A, Tarner IH, Bohle RM *et al.* Analysis of vascular gene expression in arthritis synovium by laser-mediated microdissection. Arthritis Rheum 2007; 56:1094–105.
16 Hofbauer M, Wiesener S, Babbe H *et al.* Clonal tracking of autoaggressive T cells in polymyositis by combining laser microdissection, single-cell PCR, and CDR3-spectratype analysis. Proc Natl Acad Sci USA 2003; 100:4090–5.
17 Peterson KS, Huang JF, Zhu J *et al.* Characterization of heterogeneity in the molecular pathogenesis of lupus nephritis from transcriptional profiles of laser-captured glomeruli. J Clin Invest 2004; 113:1722–33.
18 Fries JW, Roth T, Dienes HP, Weber M, Odenthal M. A novel evaluation method for paraffinized human renal biopsies using quantitative analysis of microdissected glomeruli and VCAM-1 as marker of inflammatory mesangial cell activation. Nephrol Dial Transplant 2003; 18:710–6.
19 Chan RW, Lai FM, Li EK *et al.* Intrarenal cytokine gene expression in lupus nephritis. Ann Rheum Dis 2007; 66:886–92.
20 Todd R, Margolin DH. Challenge of single-cell diagnostics: analysis of gene expression. Trends Mol Med 2002; 8:254–7.
21 Weening JJ, D'Agati VD, Schwartz MM *et al.* The classification of glomerulonephritis in systemic lupus erythematosus revised. J Am Soc Nephrol 2004; 15:241–50.
22 Weening JJ, D'Agati VD, Schwartz MM *et al.* The classification of glomerulonephritis in systemic lupus erythematosus revised. Kidney Int 2004; 65:521–30.
23 Churg J, Bernstein J, Glassock RJ. Renal disease: classification and atlas of glomerular disease, 2nd edn. Tokyo: Igaku-Shoin, 1995.
24 Bombardier C, Gladman DD, Urowitz MB, Caron D, Chang CH. Derivation of the SLEDAI. Arthritis Rheum 1992; 35:630–40.
25 Austin HA 3rd, Muenz LR, Joyce KM, Antonovych TT, Balow JE. Diffuse proliferative lupus nephritis: identification of specific pathologic features affecting renal outcome. Kidney Int 1984; 25:689–95.
26 Wang B, Esche C, Mamelak A, Freed I, Watanabe H, Sauder DH. Cytokine knockouts in contact hypersensitivity research. Cytokine Growth Factor Rev 2003; 14:381–9.
27 Crane IJ, Forrester JV. Th1 and Th2 lymphocytes in autoimmune disease. Crit Rev Immunol 2005; 25:75–102.
28 Matthys P, Vermeire K, Heremans H, Billiau A. The protective effect of IFN-gamma in experimental autoimmune diseases: a central role of mycobacterial adjuvant-induced myelopoiesis. J Leukoc Biol 2000; 68:447–54.
29 Haas C, Ryffel B, Le Hir M. IFN-gamma is essential for the development of autoimmune glomerulonephritis in MRL/Ipr mice. J Immunol 1997; 158:5484–91.
30 Bi Y, Liu G, Yang R. Th17 cell induction and immune regulatory effects. J Cell Physiol 2007; 211:273–8.
31 Wong CK, Ho CY, Li EK, Lam CW. Elevation of proinflammatory cytokine (IL-18, IL-17, IL12) and Th2 cytokine (IL-4) concentrations in patients with systemic lupus erythematosus. Lupus 2000; 9:589–93.
32 Dong GF, Ye R, Shi W *et al.* IL-17 induces autoantibody overproduction and peripheral blood mononuclear cell overexpression of IL-6 in lupus nephritis patients. Chin Med J 2003; 116:543–8.
33 Crispín JC, Oukka M, Bayliss G *et al.* Expanded double negative T cells in patients with systemic lupus erythematosus produce IL-17 and infiltrate the kidneys. J Immunol 2008; 181:8761–6.
34 Zhang C, Zhang J, Yang B, Wu C. Cyclosporine A inhibits the production of IL-17 by healthy individuals and patients with rheumatoid arthritis. Cytokine 2008; 42:345–52.
35 Cho ML, Ju JH, Kim KW *et al.* Cyclosporine A inhibits IL-15-induced IL-17 production in CD4+ T cells via down-regulation of PI3K/Akt and NF-κB. Immunol Lett 2007; 108:88–96.
36 Wong CK, Lit LC, Tam LS, Li EK, Wong PT, Lam CW. Hyperproduction of IL-23 and IL-17 in patients with systemic lupus erythematosus: implications for Th17-mediated inflammation in auto-immunity. Clin Immunol 2008; 127:385–93.
37 Yang J, Chu Y, Yang X *et al.* Th17 and natural Treg cell population dynamics in systemic lupus erythematosus. Arthritis Rheum 2009; 60:1472–83.
38 Doreau A, Belot A, Bastid J *et al.* Interleukin 17 acts in synergy with B cell-activating factor to influence B cell biology and the pathophysiology of systemic lupus erythematosus. Nat Immunol 2009; 10:778–85.
39 Nakae S, Iwakura Y, Suto H, Galli SJ. Phenotypic differences between Th1 and Th17 cells and negative regulation of Th1 cell differentiation by IL-17. J Leukoc Biol 2007; 81:1258–68.
40 Harrington LE, Hatton RD, Mangan PR *et al.* Interleukin 17-producing CD4+ effector T cells develop via a lineage distinct from the T helper type 1 and 2 lineages. Nat Immunol 2005; 6:1123–32.
41 Park H, Li Z, Yang XO *et al.* A distinct lineage of CD4 T cells regulates tissue inflammation by producing interleukin 17. Nat Immunol 2005; 6:1133–41.
42 Chu CQ, Swart D, Alcorn D, Tocker J, Elkon KB. Interferon-gamma regulates susceptibility to collagen-induced arthritis through suppression of interleukin-17. Arthritis Rheum 2007; 56:1145–51.

Available online http://arthritis-research.com/content/11/4/R118

Research article

Open Access

Tumor necrosis factor α-induced adipose-related protein expression in experimental arthritis and in rheumatoid arthritis

Asuka Inoue[1], Isao Matsumoto[1,2], Yoko Tanaka[1], Keiichi Iwanami[1], Akihiro Kanamori[3], Naoyuki Ochiai[3], Daisuke Goto[1], Satoshi Ito[1] and Takayuki Sumida[1]

[1]Division of Clinical Immunology, Advanced Biomedical Applications, Graduate School of Comprehensive Human Sciences, University of Tsukuba, 1-1-1 Tennodai, Tsukuba 305-8575, Japan
[2]PRESTO, Japan Science and Technology Agency, 4-1-8 Honcho Kawaguchi, Saitama 332-0012, Japan
[3]Department of Orthopedic Surgery, Advanced Biomedical Applications, Graduate School of Comprehensive Human Sciences, University of Tsukuba, 1-1-1 Tennodai, Tsukuba 305-8575, Japan

Corresponding author: Isao Matsumoto, ismatsu@md.tsukuba.ac.jp

Received: 6 Feb 2009 Revisions requested: 11 Mar 2009 Revisions received: 1 Aug 2009 Accepted: 6 Aug 2009 Published: 6 Aug 2009

Arthritis Research & Therapy 2009, 11:R118 (doi:10.1186/ar2779)
This article is online at: http://arthritis-research.com/content/11/4/R118

Abstract

Introduction Tumor necrosis factor-alpha (TNFα) plays a pivotal role in rheumatoid arthritis (RA); however, the mechanism of action of TNFα antagonists in RA is poorly defined. Immunization of DBA/1 mice with glucose-6-phosphate isomerase (GPI) induces severe acute arthritis. This arthritis can be controlled by TNFα antagonists, suggesting similar etiology to RA. In this study, we explored TNFα-related mechanisms of arthritis.

Methods First, we performed GeneChip analysis using splenocytes of mice with GPI-induced arthritis. Expression of TNFα-induced adipose-related protein (TIARP) mRNA and protein in spleens, joints and lymph nodes was evaluated, and fluctuation of TIARP mRNA was analyzed after administration of anti-TNFα monoclonal antibody (mAb). Localization of TIARP in spleen and joints was also explored. Six-transmembrane epithelial antigen of the prostate (STEAP) families of proteins, the human ortholog of TIARP gene, were also evaluated in human peripheral blood mononucleocytes and synovium.

Results Among the arrayed TNFα-related genes, the expression of TIARP mRNA was the highest (more than 20 times the control). TIARP mRNA was detected specifically in joints and spleens of arthritic mice, and their levels in the synovia correlated with severity of joint swelling. Treatment with anti-TNF mAb significantly reduced TIARP mRNA expression in splenocytes. Among the splenocytes, $CD11b^+$ cells were the main source of TIARP mRNA. Immunohistochemistry showed that TIARP protein was mainly localized in hyperplastic synovium. Among the STEAP family of proteins, STEAP4 was highly upregulated in joints of patients with RA and especially co-localized with $CD68^+$ macrophages.

Conclusions The results shed light on the new mechanism of action of TNFα antagonists in autoimmune arthritis, suggesting that TIARP plays an important role in inflammatory arthritis, through the regulation of inflammatory cytokines.

Introduction

Rheumatoid arthritis (RA) is a chronic inflammatory disorder with a variable disease outcome and is characterized by inflammation of multiple joints. The prognosis of RA patients has improved significantly in recent years after the introduction of tumor necrosis factor-alpha (TNFα)-based therapy [1]. Despite the wide use of these biologics, their precise mechanisms of action in RA remain unclear.

Several animal models of RA have been described; however, the therapeutic benefits of TNF antagonists have been confirmed in only a few of these models. Schubert and colleagues

CFA: complete Freund's adjuvant; ELISA: enzyme-linked immunosorbent assay; GAPDH: glyceraldehydes-3-phosphate dehydrogenase; GEO: Gene Expression Omnibus; GPI: glucose-6-phosphate isomerase; GST: glutathione S-transferase; HRP: horseradish peroxidase; IL-6: interleukin-6; mAb: monoclonal antibody; MACS: magnetic-activated cell sorting; MW: molecular weight; OA: osteoarthritis; PBMC: peripheral blood mononuclear cell; PBS: phosphate-buffered saline; PCR: polymerase chain reaction; RA: rheumatoid arthritis; STEAP: six-transmembrane epithelial antigen of the prostate; TIARP: tumor necrosis factor alpha-induced adipose-related protein; TNF: tumor necrosis factor; TNFR: tumor necrosis factor receptor.

[2] reported that continuous injections of human TNF receptor (TNFR) p75-IgG-Fc fusion protein (Etanercept) from days 0 to 9 completely protected against the development of arthritis in glucose-6-phosphate isomerase (GPI)-induced arthritis. In this regard, we recently demonstrated a clear therapeutic effect of anti-TNF monoclonal antibody (mAb) in mice with GPI-induced arthritis, and the therapeutic response correlated with the *in vitro* regulation of TNF production [3]. We also identified that anti-interleukin-6 (IL-6) receptor mAb blocks the development of GPI-induced arthritis [3,4]. These results indicate that the GPI-induced arthritis model is suitable for studying the mechanisms of action of TNFα antagonists as well as IL-6 antagonists in RA patients.

Using such a TNFα-dependent arthritis model, we investigated TNFα-related molecules by GeneChip analysis. The expression of TNFα-induced adipose-related protein (TIARP) was the highest in GeneChip study. TIARP was identified as a transmembrane protein that is highly regulated by TNFα in adipocytes [5]. Not only TNFα but also IL-6 regulated the expression of TIARP [6], suggesting the involvement of the inflammatory cascade in RA. To our knowledge, however, no information on its role in arthritis or its localization in joints has been published.

To explore the role of TIARP in arthritis, we conducted the present study in GPI-induced arthritis. TIARP mRNA and proteins were upregulated in joints and spleens in mice with GPI-induced arthritis. Administration of anti-TNFα mAb reduced TIARP mRNA in splenocytes. In arthritic mice, TIARP mRNA was expressed mainly in CD11b$^+$ cells in the spleen, and TIARP mRNA level was increased in the joints (accompanied by joint swelling), especially in hyperplastic synovium. Overexpression of the human TIARP counterpart, such as six-transmembrane epithelial antigen of the prostate-4 (STEAP4), was noted in the synovia of patients with RA. The results provide the first characterization of the role of TIARP in inflammatory arthritis.

Materials and methods

Glucose-6-phosphate isomerase-induced arthritis

Male DBA/1 mice (6 to 8 weeks old) were obtained from Charles River Laboratories (Yokohama, Japan). Recombinant human GPI was prepared as described previously [7]. Mice were immunized by intradermal injection of 300 μg of recombinant human GPI-GST (glutathione S-transferase) (hGPI) in emulsified complete Freund's adjuvant (CFA) (Difco Laboratories Inc., now part of Becton Dickinson and Company, Franklin Lakes, NJ, USA). Control mice were immunized with 100 μg of GST in CFA. Arthritic animals were assessed visually, and changes in each paw were scored on a scale of 0 to 3. A score of 0 indicates no evidence of inflammation, 1 indicates subtle inflammation or localized edema, 2 indicates swelling that is easily identified but localized to the dorsal or ventral surface of paws, and 3 indicates swelling on all aspects of paws, and the maximum possible score was 12 per mouse. The experimental protocol was approved by the Ethics Review Committee for Animal Experimentation of the University of Tsukuba (Japan).

GeneChip analysis of splenocytes from glucose-6-phosphate isomerase-induced arthritis

The spleens of three GPI-GST (molecular weight [MW] = 89 kDa) (300 μg)-immunized DBA/1 mice were harvested on day 10. As a control, the spleens of three GST (MW = 26 kDa) (100 μg)-immunized DBA/1 mice were used. Total RNA was extracted from the splenocytes using ISOGEN (Nippon Gene Co., Ltd., Toyama, Japan), and then 15 μg of RNA was used for cDNA synthesis by reverse transcription followed by synthesis of biotinylated cRNA through *in vitro* transcription. After cRNA fragmentation, hybridization with mouse 430A2.0 GeneChip (Affymetrix, Santa Clara, CA, USA) with probes for 43,000 mouse gene ESTs (expressed sequence tags) was performed in accordance with the protocol provided by the manufacturer. Analysis was performed by gene expression software.

Analysis of TIARP and tumor necrosis factor-alpha gene expression

Spleens and lymph nodes were isolated, cut into small pieces, and passed through cell strainers (BD Biosciences, Erembodegem, Belgium) to obtain single-cell suspensions. The remaining cells were washed twice with phosphate-buffered saline (PBS). Synovial tissues from the ankle joints were isolated and minced by scissors. Total RNA was extracted with ISOGEN in accordance with the instructions provided by the manufacturer. cDNA was obtained by reverse transcription with a commercially available kit (Fermentas, Glen Burnie, MD, USA). Primers sequenced were as follows: TIARP sense 5'-AGCCCACGTGGTCAAAGCAT-3' and antisense 5'-CCTTGGTCCAGTGGGGTGA-3' and glyceraldehydes-3-phosphate dehydrogenase (GAPDH) sense 5'-CGTCCCGTAGACAAAATGGT-3' and antisense 5'-GAATTTGCCGTGAGTGGAGT-3'.

All polymerase chain reactions (PCRs) were performed in a Takara PCR Thermal Cycler (Takara Bio Inc., Shiga, Japan). After denaturation at 95°C for 5 minutes, cycles were set at 10 seconds at 94°C, 10 seconds at 60°C, and 30 seconds at 72°C. Cycling was followed by 10 minutes of elongation at 72°C. PCR products were subjected to electrophoresis in 1% agarose gels in Tris-borate-EDTA (ethylenediaminetetraacetic acid) electrophoresis buffer, stained with ethidium bromide, and detected by ultraviolet transillumination. cDNA samples were normalized for the housekeeping gene *GAPDH*.

For real-time PCR, we used a TaqMan Assay-on-Demand gene expression product (Applied Biosystems, Foster City, CA, USA). The expression levels of TIARP, TNFα, and GAPDH (assay ID Mm00475402_m1, Mm00443258_m1, and Mm99999915_g1, respectively; Applied Biosystems) were

normalized relative to the expression of GAPDH. Analysis was performed with an ABI Prism 7500 apparatus (Applied Biosystems) under the following conditions: inactivation of possible contaminating amplicons with AmpErase UNG for 2 minutes at 50°C, initial denaturation for 10 minutes at 95°C, followed by 45 thermal cycles of 15 seconds at 95°C and 60 seconds at 60°C. The serum TNFα level was measured by an enzyme-linked immunosorbent assay (ELISA) kit (eBioscience, Inc., San Diego, CA, USA). After conditioning, the detection limit of TNFα concentration was 2 μg/mL.

Preparation of anti-TIARP and anti-STEAP4 antibodies

One rabbit was immunized subcutaneously by TIARP peptide$_{5-19}$ (HADEFPLTTDSSEKQ, amino-terminal peptide coupled to keyhole limpet hemocyanin) or human ortholog STEAP4 peptide$_{3-15}$ (KTCIDALPLTMNS) [8] with CFA four times, on days 0, 14, 28, and 42. The rabbit was sacrificed on day 52, and serum was collected. Serum was first purified by protein A column and then affinity-purified by TIARP-peptide$_{5-19}$ or STEAP4 peptide$_{3-15}$ column. The purified fraction was confirmed by TIARP peptide$_{5-19}$ or STEAP4 peptide$_{3-15}$ ELISA.

Western blotting

The cells were washed with PBS and incubated with lysis buffer (pH 7.4, 50 mM Tris-HCl, 5 mM $MgCl_2$, 2 mM phenylmethylsulfonyl fluoride [PMSF], and 0.5% NP-40). Where indicated, protein concentrations were quantified using the bicinchoninic acid reagent (Pierce, Rockford, IL, USA). Samples (10 μg of total protein) were separated by SDS-PAGE (4/20% acrylamide; Daiichi Pure Chemicals Co., Ltd., Tokyo, Japan) and transferred to polyvinylidene fluoride membranes (Bio-Rad Laboratories, Inc., Hercules, CA, USA). All subsequent wash buffers contained 0.05% Tween-20 in PBS. Four percent Block Ace (Dainippon Pharmaceutical, Osaka, Japan) was used to block the membranes and to dilute antibodies. Rabbit polyclonal anti-TIARP antibodies and rabbit anti-actin antibodies (Sigma-Aldrich, Munich, Germany) were used at 1:3,000 dilution. Horseradish peroxidase (HRP)-conjugated anti-rabbit secondary antibodies (1:6,000 dilution; Bio-Rad Laboratories, Inc.) were used to visualize bound anti-TIARP antibodies or anti-actin antibodies with the ECL [enhanced chemiluminescence] Western blot detection kit (Amersham, now part of GE Healthcare, Little Chalfont, Buckinghamshire, UK).

Treatment with anti-tumor necrosis factor-alpha monoclonalantibody

We used commercially available anti-TNFα mAb (eBioscience, Inc.). For a control antibody, we used similar amounts of rat IgG1 isotype control (R&D Systems, Inc., Minneapolis, MN, USA). Just after the onset of arthritis (on day 8), a single dose of 100 μg of anti-TNFα mAb or control antibody was injected. Spleen was harvested at the indicated time points and analyzed for TIARP expression. Three independent experiments were performed.

Identification of TIARP-positive cells in splenocytes of mice with glucose-6-phosphate isomerase-induced arthritis

The spleens were harvested on day 12 after GPI immunization and single-splenocyte cell suspensions were prepared as described above. CD4$^+$, CD19$^+$, CD11b$^+$, and CD11c$^+$ cells from splenocytes were isolated by magnetic beads using the MACS™ [magnetic-activated cell sorting] system (Miltenyi Biotec, Bergisch Gladbach, Germany). The cells contained more than 97% CD4$^+$, CD19$^+$, CD11b$^+$, and CD11c$^+$ cells as confirmed by fluorescence-activated cell sorting analysis. The cells were dispensed at 1 × 10^6 cells to analyze the expression of TIARP mRNA.

Immunohistochemical staining for TIARP/STEAP4

At the indicated time points, the ankles of the mice were removed, fixed, decalcified, and paraffin-embedded. Sections (5-μm thick) were stained with hematoxylin and eosin and were evaluated for histological changes. For immunohistochemical study, endogenous peroxidase activity was inhibited using 3% hydrogen peroxidase in methanol. Sections were blocked by 5% bovine serum albumin in PBS for 10 minutes and then incubated with rabbit anti-TIARP antibody (1:100 dilution) or normal rabbit Ig (1:100 dilution; Dako, Tokyo, Japan). Isotype-matched HRP-conjugated anti-rabbit IgG antibody (Bio-Rad Laboratories, Inc.) was added for 30 minutes. HRP activity was detected using 3,3-diaminobendine (DAB) (Nichirei Corporation, Tokyo, Japan) as a substrate. The stained sections were counterstained with Mayer's hematoxylin for 10 seconds and mounted with aqueous mounting medium.

For human STEAP4 staining, synovial tissues were obtained after informed consent was given by RA patients at the time of joint replacement. All RA patients satisfied the classification criteria of the American College of Rheumatology (1987) [9]. The synovium was embedded in optimal cutting temperature compound and frozen in dry ice isopentane, and 5-μm-thick sections were mounted at -25°C. Anti-human STEAP4 polyclonal antibody conjugated with fluorescein isothiocyanate (FITC protein labeling kit; Pierce) and purified anti-human CD68 (BD Pharmingen, San Diego, CA, USA) conjugated with rhodamine (1:100 dilution, Rhodamine protein labeling kit; Pierce) were used. Nuclei were counterstained with 4'-6'-diamidine-2-phenylindole dihydrochloride (DAPI) (Molecular Probes, Inc., now part of Invitrogen Corporation, Carlsbad, CA, USA). The stained sections were examined under a fluorescent microscope (model FW4000; Leica Microsystems, Tokyo, Japan).

Patients and analysis of human peripheral blood mononuclear cells and synovium for STEAP proteins

Peripheral blood mononuclear cells (PBMCs) from three female patients with RA and three healthy control subjects were obtained. All RA patients satisfied the classification criteria of the American College of Rheumatology (1987) [9]. Synovial tissues from 36 RA and 19 osteoarthritis (OA) patients were obtained at the time of total knee replacement. Written informed consent was obtained from all subjects, and the study was approved by the ethics review committee. Total RNA was extracted with ISOGEN in accordance with the protocol provided by the manufacturer. cDNA was obtained by reverse transcription with a commercially available kit. The following primers were used: STEAP2 sense 5'-CCTACAGCCTCTGCTTACCG-3' and antisense 5'-GAGGGCAAAACAAGAGCAAG-3', STEAP3 sense 5'-GCCAGAAGAGATGGACAAGC-3' and antisense 5'-GGTGCTCTTGCTCTGTAGGG-3', STEAP4 sense 5'-GCTCTCCAGTCAGGAGCACT-3' and antisense 5'-CACACAGCACAGCAGACAAA-3', and GAPDH sense 5'-GAAGGTGAAGGTCGGAGTC-3' and antisense 5'-GAAGATGGTGATGGGATTTC-3'. For real-time PCR, we used a TaqMan Assay-on-Demand gene expression product (Applied Biosystems). The expression level of STEAP4 was normalized relative to the expression of GAPDH. Methods were described above.

Statistical analysis

All data were expressed as mean ± standard error of the mean. Differences between groups were examined for statistical significance using the Mann-Whitney *U* test. A *P* value of less than 0.05 denoted the presence of a statistically significant difference.

Results

Induction of glucose-6-phosphate isomerase-induced arthritis

DBA/1 mice were immunized using the human recombinant GPI as reported previously [3,4]. All mice developed arthritis after immunization with 300 μg of GPI. Arthritis was documented at day 8, and severe arthritis was recorded at day 14, with ankle swelling reaching a maximum at day 14 but subsiding gradually on follow-up.

Overexpression of tumor necrosis factor-induced adipose-related protein in splenocytes of arthritic mice

To explore TNF-related genes in GPI-induced arthritis, we performed GeneChip analysis using arthritic splenocytes and control-immunized splenocytes. Among the arrayed TNFα-related genes, TIARP mRNA was highly expressed in arthritic splenocytes, with levels exceeding more than 20 times those of the control splenocytes (Figure 1). This finding suggests that TIARP protein is an important molecule in TNFα-dependent arthritis. The data discussed in this publication have been deposited in the Gene Expression Omnibus (GEO) of the National Center for Biotechnology Information (Bethesda, MD, USA) and are accessible through GEO Series accession number [GEO:GSE17272] [10].

Figure 1

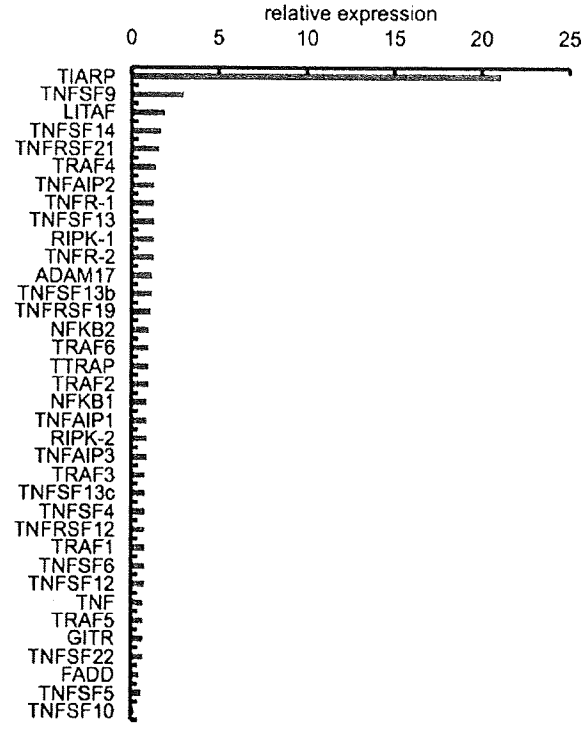

Upregulation of tumor necrosis factor-alpha (TNFα)-related genes in splenocytes of mice with glucose-6-phosphate isomerase (GPI)-induced arthritis. The mRNA expression levels of TNF-related genes in splenocytes of mice with GPI-induced arthritic (at day 10) relative to control splenocytes are shown. TNFα-induced adipose-related protein (TIARP) was specifically and strongly induced in splenocytes. GeneChip analysis was performed by gene expression software. ADAM17, a disintegrin and metallopeptidase domain 17; FADD, Fas (tumor necrosis factor receptor superfamily 6)-associated via death domain; GITR, glucocorticoid-induced tumor necrosis factor-related protein-D mRNA; LITAF, lipopolysaccharide-induced tumor necrosis factor-alpha factor; NFKB1, nuclear factor kappa B subunit p105; NFKB2, nuclear factor kappa B subunit p100; RIPK, receptor (tumor necrosis factor receptor superfamily)-interacting serine-threonine kinase 1 and 2; TNFAIP, tumor necrosis factor alpha-induced protein; TNFR, tumor necrosis factor receptor; TNFRSF, tumor necrosis factor receptor superfamily; TNFRSF12, WSL-1-like protein; TNFRSF22, tumor necrosis factor receptor family member SOBa mRNA; TNFSF, tumor necrosis factor (ligand) superfamily; TRAF, tumor necrosis factor receptor-associated factor; TTRAP, tumor necrosis factor receptor-associated factor and tumor necrosis factor receptor-associated protein.

Tumor necrosis factor-alpha and TIARP expression in glucose-6-phosphate isomerase-induced arthritis

To determine the correlation between TNFα and TIARP in GPI-induced arthritis, the time course of TIARP expression was analyzed. Serum TNFα levels were elevated at day 7

(onset of arthritis, $P < 0.05$), were at the same elevated levels at day 14 (peak of arthritis), and then subsided to the basal level at day 28 (Figure 2a). In contrast, the TNFα mRNA expression level in arthritic joints tended to increase at day 7, though insignificantly, in mice with GPI-induced arthritis. The expression level decreased later to basal levels (Figure 2b).

Both real-time PCR and Western blotting showed upregulation of TIARP mRNA and protein expression at day 7 in splenocytes of mice with GPI-induced arthritis (Figure 2c, left panel). In the joints of the same mice, upregulation of TIARP mRNA and protein was noted at days 14 and 28, and the expression correlated with joint swelling (Figure 2c, right

Figure 2

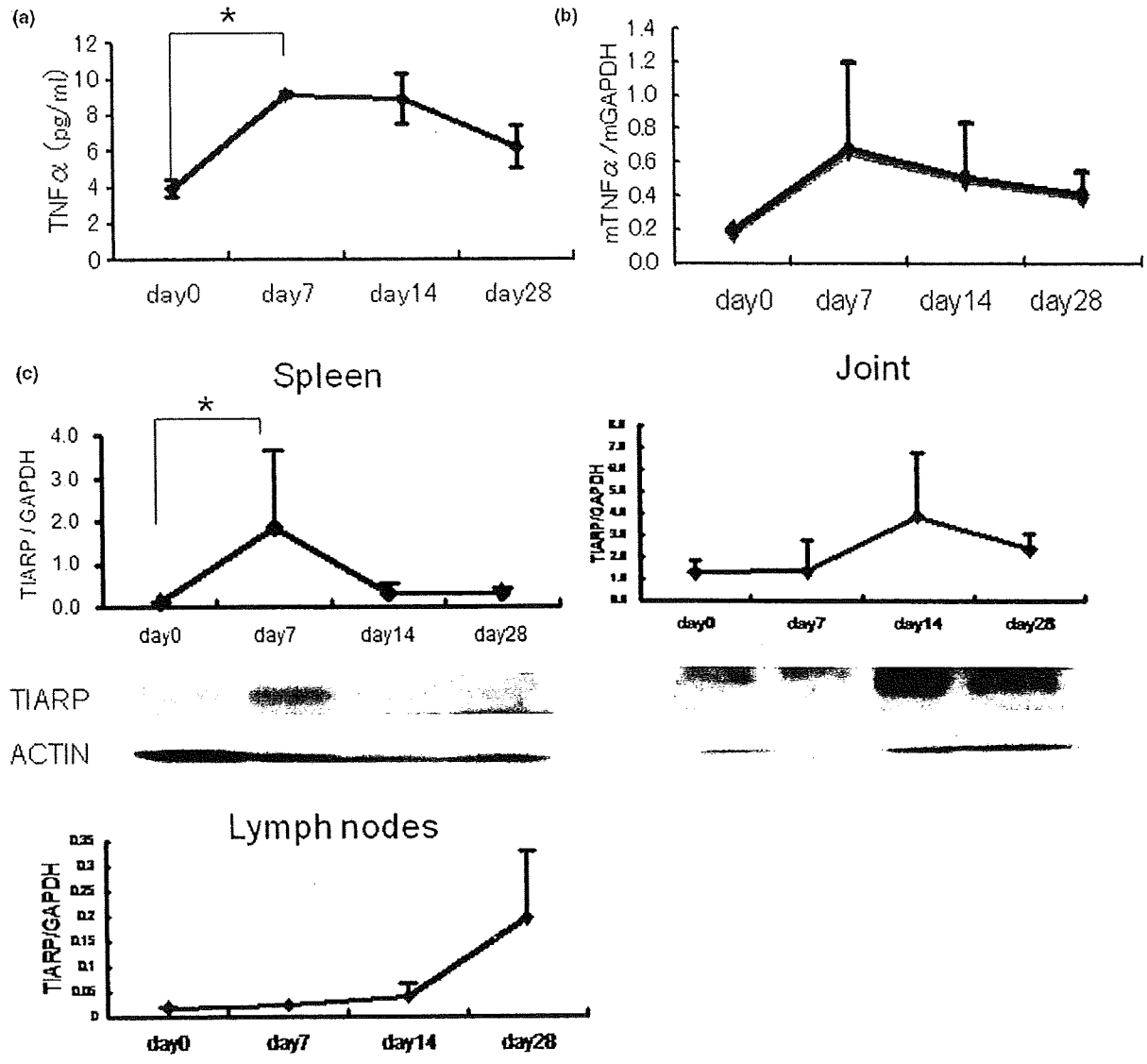

Serial changes in expression levels of tumor necrosis factor-alpha (TNFα) and TIARP in glucose-6-phosphate isomerase (GPI)-induced arthritis. Serial changes in TNFα concentrations in **(a)** serum and **(b)** arthritic joints and **(c)** TIARP mRNA and protein expression in spleens (left and middle panels) and arthritic joints (right panel) by real-time polymerase chain reaction (PCR) and Western blotting in mice with GPI-induced arthritis. As shown in the bottom panel of **(c)**, TIARP mRNA in lymph nodes was also analyzed. Arthritis appeared on days 7 and 8, peaked in severity on day 14, and then gradually subsided. High expression levels of TIARP mRNA and proteins were detected in splenocytes on day 7 (the onset of arthritis). In joints, the expression of TIARP mRNA and protein was correlated with joint swelling (days 14 and 28). Data are mean ± standard error of the mean of five mice per group. *$P < 0.05$ (Mann-Whitney *U* test). GAPDH, glyceraldehydes-3-phosphate dehydrogenase; mTNFα, murine tumor necrosis factor-alpha; TIARP, tumor necrosis factor alpha-induced adipose-related protein.

panel). Moreover, in lymph nodes, TIARP mRNA was upregulated at day 28. But the expression of TIARP mRNA in lymph nodes was very weak compared with the other tissues (Figure 2c, bottom panel). We also confirmed that the mRNA expression of TIARP in joints was upregulated at day 28, but not at day 14, in mice with collagen-induced arthritis and that expression correlated with joint swelling (data not shown). These findings suggest that the systemic upregulation of TNFα and TIARP is involved in the early phase of the disease and that TIARP expression in arthritic joints seems to correlate with joint swelling.

Treatment with anti-tumor necrosis factor-alpha monoclonal antibody suppresses TIARP expression

To test the therapeutic efficacy of anti-TNFα mAb, we injected anti-TNFα mAb after clinical onset of arthritis at day 8. A single injection of 100 μg of anti-TNFα mAb at day 8 ameliorated the disease, as indicated by a rapid fall in the semiquantitative score of arthritis (Figure 3a) [3]. To explore the relevance of the therapeutic effect of anti-TNFα mAb on TIARP expression, we evaluated TIARP expression after injection of anti-TNFα mAb in mice with GPI-induced arthritis. Treatment of mice with anti-TNFα mAb resulted in downregulation of TIARP expression in spleen relative to control Ig injection, although no treatment-related change in TIARP expression was noted at day 14 ($P = 0.03$) (Figure 3b, top panel). However, in joints, expression of TIARP mRNA was almost comparable between the treatment with anti-TNFα mAb and control Ig. These results suggest that TNF antagonism induces TIARP downregulation and results in the amelioration of arthritis.

CD11b$^+$ cells are the main source of TIARP mRNA in splenocytes of arthritic mice

In the next set of experiments, splenocytes of arthritic mice were separated into CD4$^+$, CD19$^+$, CD11b$^+$, and CD11c$^+$ cells by MACS. In naïve mice, CD19$^+$, CD11b$^+$, and CD11c$^+$ cells expressed TIARP, and induction of arthritis was associated with upregulation of TIARP mRNA in CD11b$^+$ cells, as demonstrated by quantitative PCR ($P < 0.05$ at day 7) (Figure 4a). These findings suggest the induction of TIARP in CD11b$^+$ cells in splenocytes of arthritic mice, especially during the early phase of the disease.

Localization of TIARP protein in proliferative synovium

Next, immunohistochemical analysis was conducted to determine the distribution of TIARP in the arthritic joints. For this purpose, we generated polyclonal anti-TIARP antibodies using rats, as described previously [5]. TIARP protein was clearly identified in the proliferative synovium of arthritic joints of mice (at day 14) (Figure 4b, top panels), whereas almost no signal was detected in naïve mice (Figure 4b, bottom panels). While these findings indicate TIARP protein expression in the synovium, the results do not link such expression with an ameliorative or damaging effect on the synovium.

Overexpression of STEAP4 in joints of rheumatoid arthritis patients and its localization in CD68$^+$ cells

To determine the role of STEAP4 (the human ortholog of mouse TIARP)in human RA, we analyzed PBMCs from RA patients and healthy subjects and synovia from RA patients. For comparison, we also screened other STEAP family members such as STEAP2 and STEAP3 using the same method. For PBMCs, STEAP4 mRNA was detected in only one RA patient (1/3). Importantly, STEAP4 mRNA was highly expressed in all four RA synovia whereas only faint bands were noted for other STEAP families (Figure 5a). Next, using several numbers of synovial tissues from patients with RA and OA, we investigated the expression of STEAP4 mRNA in synovium of patients with RA and OA. Relative expression of STEAP4 was almost comparable between RA and OA, although expression variation tended to be enhanced in RA synovium (Figure 5b). Moreover, immunohistochemical analysis of synovia of RA patients showed co-localization of STEAP4 protein with CD68, a marker for human macrophages (Figure 5c). These findings suggest that STEAP4 is specifically expressed in joints and is localized with CD68$^+$ cells.

Discussion

Although the therapeutic effect of TNF antagonists is confirmed in RA [1], only a few animal models of arthritis have been used to confirm the beneficial effects of TNF antagonists. For example, a recent study reported the therapeutic effect of anti-TNF mAb in DNaseII, type I interferon receptor (IFN-IR) double-knockout mice [11], although this was not a genetically unaltered mouse. Furthermore, Schubert and colleagues reported the protective effect of TNF antagonist in GPI-induced arthritis [2] and arthritis was clearly B cell-dependent [12]. We recently demonstrated the therapeutic effect of TNF antagonist in GPI-induced mice. Thus, it is important to explore TNF-regulated genes in the latter model to understand the mechanisms of action of TNFα antagonists in RA patients. When the GeneChip analysis was used, the present results showed upregulation of TIARP mRNA in the spleen of arthritic mice. TIARP was first identified as TNFα-induced cell surface protein in adipose tissues and is also known to be localized in the liver, kidney, heart, and skeletal muscle [5]. This protein was detected in the course of adipocyte differentiation and conversion and is also induced by IL-6 [6]. In this study, we confirmed its induction in CD11b$^+$ splenocytes in arthritis and we confirmed that it is upregulated in the arthritic synovium of murine GPI-induced arthritis. These findings suggest the involvement of TIARP in the process of proliferation or differentiation state induced by inflammation. In fact, previous studies indicated that TIARP is induced by TNFα and IL-6 in adipocytes [5,6]. TNFα and IL-6 are pleiotropic cytokines known to play crucial roles in human RA, and significant therapeutic effects of their antagonists have been confirmed in recent years [1,13]. In GPI-induced arthritis, both TNFα and IL-6 antagonists have protective effects [3,4], and these cytokines play important roles in the induction of arthritis in col-